VAN DER WALT, DAVID MICHAEL

EXTENSIONS OF BCS THEORY FOR NON-CONVENTIONAL SUPERCONDUCTORS

MSc UP 1993

Extensions of BCS theory for non-conventional superconductors

by

David Michael van der Walt

Submitted in partial fulfillment of the requirements for the degree
Magister Scientiae (Physics)
in the Faculty of Science
University of Pretoria
Pretoria
December 1993

Extensions of BCS theory for non-conventional superconductors

D M van der Walt

Extensions of BCS theory for non-conventional superconductors

by
David Michael van der Walt

Submitted in partial fulfillment of the requirements for the degree
Magister Scientiae (Physics)
in the department of Physics
Faculty of Science
University of Pretoria

Supervisor : Dr R M Carter

The Bardeen-Cooper-Schrieffer (BCS) theory of superconductivity affords a very good microscopic understanding of metallic superconductors, where the electron-electron interaction is known to be phonon-mediated. However, it does not adequately describe non-conventional, in particular high-T_c, superconductivity.

In this dissertation, BCS theory has been extended in an attempt to provide a framework within which the mechanisms responsible for exotic superconductivity can be understood. The BCS gap equation is solved without the usual restriction of small interaction width for the intermediating bosons, since the electron-electron interaction responsible for superconductive pairing need not necessarily be phonon mediated.

Bulk high-T_c superconductors are usually polycrystalline materials, composed of weakly coupled grains which may as a first approximation be treated as small isolated superconducting systems. The finite size of these individual grains needs to be taken into account in an effective description of high temperature superconductivity. Nuclei that exhibit a BCS-type pairing transition also fall into the category of small superconducting systems. For these finite systems, the effect of the thermodynamic and quantum fluctuations needs to be included. In particular, the effect of fluctuations on the macroscopic order parameter of the system, which drops smoothly to zero in the

thermodynamic limit to indicate a phase transition, is examined. Furthermore, the expectation value of the pairing potential, rather than the conventional BCS energy gap, is proposed and motivated as the more appropriate order parameter for pairing systems. Finally, canonical number projection is also performed to take into account the finite number of superconducting particles in small superconducting systems.

Uitbreidings van die BCS teorie vir onkonvensionele supergeleiers

deur
David Michael van der Walt

Voorgelê ter gedeeltelike vervulling van die vereistes vir die graad
Magister Scientiae (Fisika)
in die department Fisika
Fakulteit Natuurwetenskappe
Universiteit van Pretoria

Studieleier : Dr. R M Carter

Die Bardeen-Cooper-Schrieffer (BCS) teorie vir supergeleiding bied 'n baie goeie mikroskopiese begrip van metaal-supergeleiers, waar dit bekend is dat die elektron-elektron-interaksie deur fonone bewerkstellig word. Dit slaag egter nie daarin om onkonvensionele, en in die besonder hoë-T_c supergeleiding, bevredigend te beskryf nie.

In hierdie verhandeling word BCS teorie uitgebrei in 'n poging om 'n raamwerk daar te stel waarbinne die meganismes verantwoordelik vir eksotiese supergeleiding verstaan kan word. Die BCS-gapingvergelyking word opgelos sonder die gebruiklike beperking op die interaksiebereik van die tussengangerbosone, aangesien die elektron-elektron interaksie verantwoordelik vir supergeleidende paarvorming nie noodwendig deur fonone gemediëer word nie.

Hoë temperatuur supergeleiers is in die reël polikristallyn, en word saamgestel uit swak-gekoppelde korrels wat as 'n eerste benadering as klein geïsoleerde supergeleidende sisteme beskou kan word. Die eindige grootte van die individuele korrels moet in ag geneem word in 'n effektiewe beskrywing van hoë temperatuur supergeleiding. Kerne wat 'n BCS-tipe paringsoorgang ondergaan, val ook in die kategorie van klein supergeleidende sisteme. In hierdie eindige sisteme, moet die effek van termodinamiese en kwantumfluktuasies in ag geneem word. In besonder word die effek van fluktuasies op die makroskopiese orde-parameter van die sisteem, wat in die termodinamiese

limiet na nul neig om 'n fase-oorgang aan te dui, ondersoek. Verder word die verwagtingswaarde van die paringspotensiaal, eerder as die konvensionele BCS energiegaping, voorgestel en gemotiveer as die meer toepaslike order-parameter vir paringsisteme. Ten laaste word kanoniese getalprojeksie ook uitgevoer om die eindige aantal deeltjies in klein supergeleidende sisteme in berekening te bring.

Acknowledgements

I would like to thank the following persons and institutions for their assistance in the preparation and completion of this dissertation:

My supervisor, Dr R M Carter, for continued guidance, support and encouragement, as well as financial assistance. I would particularly like to thank Dr Carter for the patient, instructive and very friendly attitude which she always had towards a sometimes less than ideal student!

The Foundation for Research Development, Pretoria, for financial support.

Dr Fritz Solms of the Rand Afrikaans University for very fruitful discussions, and permission to use Figs. 4.1 and 4.2.

Prof H G Miller of the physics department at the University of Pretoria, and Dr N J Davidson, currently at the University of Manchester, England, for useful discussions.

Prof M de Llano, North Dakota State University, for useful comments, and for proofreading parts of the manuscript.

M Marinus, a fellow student at the University of Pretoria, for proofreading the manuscript.

The department of Physics, University of Pretoria, and in particular
Prof E H Friedland, head of department, for the use of the excellent facilities at the department, and the secretarial personnel, Mrs A Schickerling, Mrs C J Vos and Mrs F M Bahula, for their friendly assistance and support.

Finally, I am indebted to L de Lange for continued support and encouragement, and for pointing out several typographical errors in the manuscript.

Contents

List of Figures

List of Tables

Chapter 1

Introduction

In 1913 Heike Kamerlingh Onnes observed that the electrical resistance of mercury dropped discontinuously to an immeasurably small value at a temperature of 4.2 K [1]. He called the new state into which the mercury had passed the *superconductive* state. At the time, he could not have imagined what a wealth of basic questions and intriguing possibilities would arise from the phenomenon of superconductivity, nor that it would not be fundamentally understood for almost half a century.

The Bardeen-Cooper-Schrieffer (BCS) theory of superconductivity [2], developed in 1957, has long been hailed as one of the major successes of modern many-body theory. Requiring just a single parameter to be fixed by comparison with experiment, namely the electron-phonon coupling constant, this microscopic theory yields excellent agreement with experiment on nearly all other properties of interest in metallic superconductors. Amongst these is the prediction of the so-called "phonon barrier", which limits the critical temperature T_c for the transition from the superconducting to the normal state, to about 40 K.

The pairing ideas developed by BCS have, with certain modifications, successfully been applied to systems other than metallic superconductors. In liquid ^{3}He, the Helium atoms forming the Cooper pair are known to be in a p-wave state with nonzero angular momentum [3, 4, 5], rather than the conventional s-wave state. Neutrons near the Fermi surface of a neutron star are also thought to suffer a BCS-type condensation [6], with p-wave pairing dominating at higher neutron density [7]. In the nuclear shell model, nucleons may be regarded as almost independent particles filling a set of shells. The

residual interactions in heavy nuclei often leads to the formation of Cooper pairs composed of nucleons of opposite angular momentum, resulting in a BCS-like pairing transition [8].

A variety of non-conventional superconductors have been discovered which do not fit the BCS mould. These include amongst others organic superconductors [9, 10], where a coherent description of the superconductive mechanism does not yet exist, and heavy-fermion metals [11], where a non-phonon mechanism may be responsible for superconductivity [3]. It was, however, with the discovery of the high-T_c copper oxide superconductors, first observed in 1986 by Bednorz and Müller [12], that the situation was radically altered. These superconductors, with critical temperatures as high as 153 K [13], defy description by conventional BCS theory.

A plethora of theories, phenomenological and otherwise, have been put forward to explain the behaviour of these exotic superconductors. One school of thought maintains that it should be possible to obtain the correct formalism within a BCS-like framework [14, 15]. Others insist that a radically new theory is required [16]. Theorists from both camps seem to agree that a pairing transition takes place at the onset of superconductivity, but differ strongly on the nature of the objects that undergo pairing, and the mechanisms responsible for the process [17, 18]. Both groups have had little success in adequately describing the physics underlying the new superconductivity, and in explaining the exotic behaviour of the oxide superconductors in both the normal and the superconducting state [17].

In this dissertation I have examined several methods of extending BCS theory in an effort to answer some of the questions arising from the discussion above. Although both Schrieffer and Anderson, at present two of the leading high-T_c theorists, agree that an understanding of the normal phase of the high-T_c superconductors must probably precede a description of the superconductive mechanism [17], I neglect entirely this aspect of the new superconductors. Also, no claim is being made that a fundamental understanding of high-T_c superconductivity has been reached. Rather the aim is to explore the consequences of removing some of the restrictions from conventional BCS theory, in the hope that the results may be applicable in the description of those forms of superconductivity which are at present incompletely or poorly understood.

Chapter 2 contains a review of microscopic BCS theory. In chapter 3 the standard BCS gap equation is solved *without* the restriction that the

interaction width of the intermediating bosons be small with respect to the Fermi energy [19, 20]. Thus possible candidates for these bosons other than phonons (which are limited by the Debye frequency) are no longer excluded. Furthermore, since the interaction is not confined to a narrow shell about the Fermi energy, the model is no longer restricted to the description of quasi-two-dimensional systems, but may be applied, at least in the weak coupling limit, to quasi-1D and to three dimensional systems. This is appropriate, since organic superconductors are sometimes modelled as one dimensional molecular chains [9], while the energy gap in heavy-fermion metal superconductors is believed to be dependent on the three dimensional momentum vector $\mathbf{k}$ [3].

BCS theory provides a mean-field description of a system, in that the system is assumed to be in its most probable state, and fluctuations into other states are ignored. For finite systems at nonzero temperature, thermal excitation may induce thermodynamic or statistical fluctuations of the system into states other than the most probable state. Non-thermodynamic fluctuations, known collectively as quantum fluctuations, also arise, primarily because the system is assumed to be in a state which is not an exact eigenstate of the system. For instance, the fact that the BCS ground state does not have good particle number violates the particle number symmetry of the exact Hamiltonian. These fluctuations can strongly affect the equilibrium distribution of finite systems.

The individual crystals or grains in polycrystalline high-T_c superconductors can be regarded as finite superconducting systems. Experimental evidence indicates that the critical current in sintered polycrystalline superconductors is about two orders of magnitude lower than in single crystals or grains [21]. This indicates that the individual grains of these materials are only weakly coupled [22, 23], and therefore they may as a first approximation be treated as isolated superconducting systems [24]. The effect of finite system size is even more pronounced in nuclei that exhibit a pairing phase transition, since here the number of nucleons is not only finite but small. In these systems, the mean-field BCS approach is insufficient, since thermodynamic and quantum fluctuations about the most probable state of the system must be taken into account. This can be done within the framework of a functional integral approach, also known as the path integral method. An outline of various existing path integral approximation schemes to the grand partition function of a system, as well as the physical interpretation

of these approximations, is therefore given in chapter 4.

In the Landau order parameter theory, the macroscopic state of a system is characterized by a macroscopic order parameter, which tends smoothly to zero in the event of a second order phase transition, such as a pairing transition. For a system in the thermodynamic limit, the concept of a phase transition is sharply defined, and an order parameter with the proper behaviour is readily chosen. It is usual in pairing systems to choose the BCS energy gap Δ for the order parameter, since, in large systems, Δ has the correct behaviour as the critical temperature T_c is approached. In finite systems, however, thermodynamic fluctuations "smooth out" the phase transition, and a sharp phase transition no longer occurs. Thus the conventional "order parameter" concept has to be reexamined. One finds that, although it is still possible to define an order parameter for a finite system, the absence of a sharp phase transition implies that the order parameter need not remain nonzero above the critical temperature. In a finite system, this is precisely the case for the BCS gap Δ, if the effect of thermal fluctuations is included. Thus Δ has traditionally been chosen as the order parameter of a system, independent of the system size.

There are, however, certain conceptual difficulties that arise when the gap is chosen as the order parameter. Firstly, if the BCS gap is momentum dependent, it is no longer a single macroscopic parameter describing the macroscopic state of the system. This criticism is valid both for a finite system, or a large system in the thermodynamic limit. Furthermore, in an exact canonical calculation in a finite system, the gap Δ is zero on both sides of the phase transition, as is easily seen from the definition of the BCS energy gap. By comparing the functional integral representation of the partition function with the Landau order parameter representation, we were led to propose the expectation value of the pairing potential, $\mathcal{G}$, as the order parameter of the system, rather than the BCS energy gap Δ [25]. Not only are the conceptual difficulties arising from the choice of Δ as the order parameter resolved, but the numerical calculations in chapter 4 indicate that the use of $\mathcal{G}$ yields better results.

The fluctuations in particle number inherent in a grand canonical calculation induce fluctuations in other observable quantities. The relative root mean square number fluctuations are of order $\frac{1}{\sqrt{N}}$, and their effect is therefore negligible in large systems. For finite systems, however, these fluctuations may be appreciable, and the calculation of the properties of a system should

take place in the canonical ensemble, where the particle number is fixed. In superconducting grains, the number of superconducting particles, although finite, is still large, and a canonical calculation is unnecessary. However, one would expect a canonical treatment to be particularly appropriate for a nuclear system that exhibits a BCS-type pairing transition, since the number of nucleons that participate in the pairing process is not only finite but small, and one expects the effect of the grand canonical number fluctuations to be of order $\frac{1}{\sqrt{N}}$.

The properties of a system are often more readily calculated in the grand canonical ensemble. The simplification achieved by the introduction of a BCS ground state which violates particle number symmetry provides a prime example. Various methods exist to project the canonical from the grand canonical results [26]. In order to test these methods, canonical number projection is performed in chapter 5. These calculations were done in the $i_{\frac{13}{2}}$ model, a simple nuclear model discussed in Appendix A. This model provides a suitable testing ground, since it allows the calculation of exact canonical and grand canonical results. Furthermore, since exact calculations are in general not possible, the projection methods were applied to an approximate grand partition function [27]. The grand partition function was approximated using a functional integral approach, with thermodynamic and small-amplitude quantum fluctuations included (see chapter 4). The projected canonical results turned out to be extremely disappointing, particularly since the path integral approximation used for the grand partition function is very good. The projected results differ from the exact canonical heat capacity by a minimum average of 10 %, which is of the same order of magnitude as the difference between the exact canonical and grand canonical results. These results suggest that even though the exact grand canonical partition function in principle contains all the information on the various canonical ensembles, this information is lost when only a good approximation to the grand partition function is known.

Chapter 6 contains a summary of the results of this dissertation, as well as some conclusions.

Chapter 2

Microscopic BCS Theory

2.1 The electron-phonon interaction and Cooper pairs

The first major step towards a microscopic understanding of metallic superconductivity came in 1950 when Fröhlich [28] suggested that the interaction between electrons and the vibrations of the positive ions forming the metallic lattice could lead to an effective interaction between the electrons themselves. This idea was soon experimentally verified with the discovery of the isotope effect, whereby the transition temperature T_c of different isotopes of the same element varies with the ionic mass M according to the relation

$$T_c \propto M^{-\frac{1}{2}} , \tag{2.1}$$

which is obeyed by most superconductors. Fröhlich also noted that, near to the Fermi surface, the interaction between the electrons via vibrational quanta or phonons is attractive, and can outweigh the Coulomb repulsion between the electrons, resulting in a net attractive interaction. It should be mentioned that the phonons which mediate the interaction are *virtual* in nature, since they only exist during the exchange between electrons, and cannot dissipate into the lattice as real phonons.

With the physical basis for an attractive electron-electron interaction established, Cooper [29] solved the Schrödinger equation for a pair of electrons of opposite momentum and spin, *in the Fermi sea*, interacting via an attractive potential. In this model, the many-particle medium serves only to

restrict the intermediate states available to the electrons. Thus the electrons may not scatter into the filled Fermi sea, in accordance with the Pauli exclusion principle. Cooper's calculation showed that the non-interacting ground state, corresponding to a filled Fermi sea, was unstable with respect to pair formation. These so called "Cooper pairs" have a finite binding energy, which results in a reduction of the total energy of the system, and provides a qualitative explanation for the gap in the excitation spectrum which is characteristic of most superconductors.

Valuable as it was, the work by Cooper neglects most of the many-body aspects of a metallic superconducting system, and is therefore incapable of describing the true ground state, which must involve many pairs. The consistent treatment of the full many-body problem was the crowning achievement of Bardeen, Cooper and Schrieffer (BCS).

2.2 Zero temperature BCS theory

The BCS Hamiltonian in second quantized form is given by

$$\begin{aligned}\hat{K} &= \hat{H} - \mu\hat{N} = \hat{T} - \mu\hat{N} + \hat{V} \\ &= \sum_{\mathbf{k},\lambda} a^{\dagger}_{\mathbf{k}\lambda} a_{\mathbf{k}\lambda} \left(\epsilon^0_k - \mu\right) - \frac{1}{2} \sum_{\substack{\mathbf{k_1}+\mathbf{k_2}=\mathbf{k_3}+\mathbf{k_4} \\ \lambda_1\lambda_2\lambda_3\lambda_4}} < \mathbf{k}_1\lambda_1\mathbf{k}_2\lambda_2|V|\mathbf{k}_3\lambda_3\mathbf{k}_4\lambda_4 > \\ &\quad \times \; a^{\dagger}_{\mathbf{k_1}\lambda_1} a^{\dagger}_{\mathbf{k_2}\lambda_2} a_{\mathbf{k_4}\lambda_4} a_{\mathbf{k_3}\lambda_3} \,, \end{aligned} \tag{2.2}$$

where $a^{\dagger}_{\mathbf{k}\lambda}$ is a creation and $a_{\mathbf{k}\lambda}$ a destruction operator for a particle with momentum $\mathbf{k}$ and spin λ, $\hat{N} = \sum_{\mathbf{k},\lambda} a^{\dagger}_{\mathbf{k}\lambda} a_{\mathbf{k}\lambda}$ is the number operator, $\epsilon^0_k = \frac{\hbar^2 k^2}{2m}$ is the free single particle energy, μ is the chemical potential, and the restricted sum in the (attractive, i.e. $V > 0$) potential term corresponds to the conservation of momentum. The introduction of the chemical potential will become clear shortly. If, in the potential term, we only consider scattering of a pair $(\mathbf{k}', \uparrow), (-\mathbf{k}', \downarrow)$ into $(\mathbf{k}, \uparrow), (-\mathbf{k}, \downarrow)$, then Eq. (2.2) reduces to

$$\hat{K} = \sum_{\mathbf{k},\lambda} a^{\dagger}_{\mathbf{k}\lambda} a_{\mathbf{k}\lambda} \left(\epsilon^0_k - \mu\right) - \sum_{\mathbf{k},\mathbf{k}'} V_{\mathbf{k}\mathbf{k}'} a^{\dagger}_{\mathbf{k}\uparrow} a^{\dagger}_{-\mathbf{k}\downarrow} a_{-\mathbf{k}'\downarrow} a_{\mathbf{k}'\uparrow} \,, \tag{2.3}$$

where

$$V_{\mathbf{k}\mathbf{k}'} = < \mathbf{k}{-}\mathbf{k}|V|\mathbf{k}'{-}\mathbf{k}' > \ . \tag{2.4}$$

We assume here that this type of scattering makes the dominant contribution to the potential term in equation (2.2), and neglect any effect of the omitted terms on the single particle energies ϵ_k^0. The justification of these and other assumptions made in deriving the BCS equations, lies ultimately in the success of the theory. The BCS ground state is now given by

$$|\Phi > = \prod_{\mathbf{k}} \left(u_k + v_k a^\dagger_{\mathbf{k}\uparrow} a^\dagger_{-\mathbf{k}\downarrow} \right) |0> \ . \tag{2.5}$$

Here $|0>$ is the no-electron state or "vacuum". The numbers u_k and v_k are real and depend only on $|\mathbf{k}|$, with $|u_k|^2$ the probability that the pair $(\mathbf{k}\uparrow), (-\mathbf{k}\downarrow)$ is unoccupied, and $|v_k|^2$ the probability that it is occupied. It is clear that the state $|\Phi>$ does not contain a fixed number of particles, since it only specifies the pair occupation probabilities. Particle number can only be conserved on the average by fixing the chemical potential such that $< \Phi|\hat{N}|\Phi >= N$, with N is the actual number of particles.

In order to apply a variational method, the expectation value of the Hamiltonian in the state $|\Phi>$ is required. It is convenient to introduce the following transformation [30]

$$\alpha_{\mathbf{k}} = u_k a_{\mathbf{k}\uparrow} - v_k a^\dagger_{-\mathbf{k}\downarrow} , \qquad \beta_{-\mathbf{k}} = u_k a_{-\mathbf{k}\downarrow} + v_k a^\dagger_{\mathbf{k}\uparrow} , \tag{2.6}$$

with the inverse transformation

$$a_{\mathbf{k}\uparrow} = u_k \alpha_{\mathbf{k}} + v_k \beta^\dagger_{-\mathbf{k}} , \qquad a_{-\mathbf{k}\downarrow} = u_k \beta_{-\mathbf{k}} - v_k \alpha^\dagger_{\mathbf{k}} . \tag{2.7}$$

The new operators must obey fermion anticommutation relations for the transformation to be canonical. This implies

$$u_k^2 + v_k^2 = 1 . \tag{2.8}$$

The expectation value $< \Phi|\hat{K}|\Phi >$ may now be evaluated by applying Wick's theorem. Define the contraction

$$\underbrace{a^\dagger_{\mathbf{k}\lambda} a_{\mathbf{k}'\lambda'}} = a^\dagger_{\mathbf{k}\lambda} a_{\mathbf{k}'\lambda'} - N\left(a^\dagger_{\mathbf{k}\lambda} a_{\mathbf{k}'\lambda'} \right) , \tag{2.9}$$

where N denotes normal ordering with respect to the operators α and β. It is readily verified that

$$\alpha_{\mathbf{k}}|\Phi> = \beta_{\mathbf{k}}|\Phi> = 0 \quad \forall\, \mathbf{k}\,, \tag{2.10}$$

and therefore the expectation value of the normal ordered product in the BCS ground state $|\Phi>$ vanishes. Since the contraction is simply a c-number, one obtains

$$\underbrace{a^{\dagger}_{\mathbf{k}\lambda} a_{\mathbf{k}'\lambda'}} = <\Phi| a^{\dagger}_{\mathbf{k}\lambda} a_{\mathbf{k}'\lambda'} |\Phi> \ . \tag{2.11}$$

The expectation value of the kinetic term of the Hamiltonian in the BCS ground state may thus be expressed as

$$<\Phi|\hat{K}_{kin}|\Phi> = \sum_{\mathbf{k}} (\epsilon^0_k - \mu)\, \underbrace{a^{\dagger}_{\mathbf{k}\uparrow} a_{\mathbf{k}\uparrow}} + \sum_{\mathbf{k}} (\epsilon^0_k - \mu)\, \underbrace{a^{\dagger}_{-\mathbf{k}\downarrow} a_{-\mathbf{k}\downarrow}} \ . \tag{2.12}$$

The contractions are

$$\begin{aligned} \underbrace{a^{\dagger}_{\mathbf{k}\uparrow} a_{\mathbf{k}\uparrow}} &= <\Phi| \left(u_k \alpha^{\dagger}_{\mathbf{k}} + v_k \beta_{-\mathbf{k}}\right) \left(u_k \alpha_{\mathbf{k}} + v_k \beta^{\dagger}_{-\mathbf{k}}\right) |\Phi> \\ &= v_k^2 \,, \end{aligned} \tag{2.13}$$

and

$$\begin{aligned} \underbrace{a^{\dagger}_{-\mathbf{k}\downarrow} a_{-\mathbf{k}\downarrow}} &= <\Phi| \left(u_k \beta^{\dagger}_{-\mathbf{k}} - v_k \alpha_{\mathbf{k}}\right) \left(u_k \beta_{-\mathbf{k}} - v_k \alpha^{\dagger}_{\mathbf{k}}\right) |\Phi> \\ &= v_k^2 \,, \end{aligned} \tag{2.14}$$

where (2.10) and the inverse transformation (2.7) have been used. Therefore

$$<\Phi|\hat{K}_{kin}|\Phi> = 2 \sum_{\mathbf{k}} \xi_k v_k^2 \,, \tag{2.15}$$

with $\xi_k = \epsilon^0_k - \mu$ the single particle energy measured with respect to the chemical potential. The expectation value of the potential, $<\Phi|\hat{K}_{pot}|\Phi>$, is given by

$$\begin{aligned} <\Phi|\hat{K}_{pot}|\Phi> \quad = \quad & \sum_{\mathbf{k},\mathbf{k}'} V_{\mathbf{k}\mathbf{k}'} \Big[\underbrace{a^{\dagger}_{\mathbf{k}\uparrow} a^{\dagger}_{-\mathbf{k}\downarrow}}\, \underbrace{a_{-\mathbf{k}'\downarrow} a_{\mathbf{k}'\uparrow}} \ + \\ & \underbrace{a^{\dagger}_{\mathbf{k}\uparrow} a_{\mathbf{k}'\uparrow}}\, \underbrace{a^{\dagger}_{-\mathbf{k}\downarrow} a_{-\mathbf{k}'\downarrow}} \ - \ \underbrace{a^{\dagger}_{\mathbf{k}\uparrow} a_{-\mathbf{k}'\downarrow}}\, \underbrace{a^{\dagger}_{-\mathbf{k}\downarrow} a_{\mathbf{k}'\uparrow}} \Big] \ . \end{aligned} \tag{2.16}$$

The contractions are

$$\begin{aligned}
\underbrace{a^{\dagger}_{\mathbf{k}\uparrow}a^{\dagger}_{-\mathbf{k}\downarrow}} &= u_k v_k \\
\underbrace{a_{-\mathbf{k}'\downarrow}a_{\mathbf{k}'\uparrow}} &= u_{k'} v_{k'} \\
\underbrace{a^{\dagger}_{\mathbf{k}\uparrow}a_{\mathbf{k}'\uparrow}} &= \underbrace{a^{\dagger}_{-\mathbf{k}\downarrow}a_{-\mathbf{k}'\downarrow}} = \delta_{\mathbf{k},\mathbf{k}'}\, v_k^2 \\
\underbrace{a^{\dagger}_{\mathbf{k}\uparrow}a_{-\mathbf{k}'\downarrow}} &= \underbrace{a^{\dagger}_{-\mathbf{k}\downarrow}a_{\mathbf{k}'\uparrow}} = 0\,, \qquad (2.17)
\end{aligned}$$

where once again (2.10) and (2.7) have been used. The nonzero contractions of the form $\underbrace{a^{\dagger}_{\mathbf{k}\uparrow}a_{\mathbf{k}'\uparrow}}$ and $\underbrace{a^{\dagger}_{-\mathbf{k}\downarrow}a_{-\mathbf{k}'\downarrow}}$ generate the Hartree-Fock (HF) self-consistent field corrections to the free single particle energy $\epsilon_k^0 = \frac{\hbar^2 k^2}{2m}$. Thus the contributions from these contractions are included by simply replacing ϵ_k^0 by $\epsilon_k = \frac{\hbar^2 k^2}{2m^*}$, the single-particle energy evaluated in the HF approximation [31, 3], with m^* the effective mass. This is useful, since the experimental values for the effective mass and density of states used in applications of the theory contain the HF corrections. The remaining terms in (2.16) may be evaluated to give

$$< \Phi|\hat{K}_{pot}|\Phi > = \sum_{\mathbf{k},\mathbf{k}'} V_{\mathbf{k}\mathbf{k}'} u_k v_k u_{k'} v_{k'}\,. \qquad (2.18)$$

Combining Eqs. (2.15) and (2.18), the following expression is obtained for the expectation value of the Hamiltonian in the BCS ground state :

$$< \Phi|\hat{K}|\Phi > = 2\sum_{\mathbf{k}} \xi_k v_k^2 - \sum_{\mathbf{k},\mathbf{k}'} V_{\mathbf{k}\mathbf{k}'} u_k v_k u_{k'} v_{k'}\,. \qquad (2.19)$$

This expression is now minimized with respect to variations of v_k, bearing in mind that by virtue of the constraint (2.8),

$$\frac{\partial u_k}{\partial v_k} = -\frac{v_k}{u_k}\,. \qquad (2.20)$$

Differentiating (2.19) gives

$$\frac{\partial}{\partial v_k} < \Phi|\hat{K}|\Phi > = 4\xi_k v_k - 2u_k \sum_{\mathbf{k}'} V_{\mathbf{k}\mathbf{k}'} u_{k'} v_{k'} + 2\frac{v_k^2}{u_k} \sum_{\mathbf{k}'} V_{\mathbf{k}\mathbf{k}'} u_{k'} v_{k'}\,, \qquad (2.21)$$

and for an extremum one requires $\frac{\partial}{\partial v_k} < \Phi|\hat{K}|\Phi >= 0$, so that

$$2\xi_k v_k u_k \; - \; \Delta_k u_k^2 \; + \; \Delta_k v_k^2 \; = \; 0 \; , \tag{2.22}$$

where we have introduced the energy gap

$$\Delta_k \; \equiv \; \sum_{\mathbf{k}'} V_{\mathbf{k}\mathbf{k}'} u_{k'} v_{k'} \; . \tag{2.23}$$

Eqs. (2.8), (2.22) and (2.23) must now be solved simultaneously for u_k, v_k and Δ_k. The constraint $u_k^2 + v_k^2 = 1$ can be incorporated by writing

$$u_k \; = \; \cos\chi_k \; , \qquad v_k \; = \; \sin\chi_k \; , \tag{2.24}$$

which reduces (2.22) to

$$\xi_k \sin 2\chi_k \; = \; \Delta_k \cos 2\chi_k \; , \tag{2.25}$$

with the solution

$$\begin{aligned} \sin 2\chi_k \; &= \; \frac{\Delta_k}{E_k} \; = \; 2u_k v_k \\ \cos 2\chi_k \; &= \; \frac{\xi_k}{E_k} \; = \; u_k^2 - v_k^2 \; . \end{aligned} \tag{2.26}$$

Here the definition

$$E_k \; \equiv \; \sqrt{\Delta_k^2 + \xi_k^2} \tag{2.27}$$

has been made, and the sign choice in (2.26) ensures that $< \Phi|\hat{K}|\Phi >$ is a minimum rather than a maximum. With this choice, Eqs. (2.26) and (2.23) become

$$\begin{aligned} u_k^2 \; &= \; \frac{1}{2}\left(1 + \frac{\xi_k}{E_k}\right) \\ v_k^2 \; &= \; \frac{1}{2}\left(1 - \frac{\xi_k}{E_k}\right) \\ \Delta_k \; &= \; \sum_{\mathbf{k}'} V_{\mathbf{k}\mathbf{k}'} \frac{\Delta_{k'}}{2E_{k'}} \; . \end{aligned} \tag{2.28}$$

This last relation is known as the BCS gap equation, and is valid for a general interaction $V_{\mathbf{kk'}}$. This equation always has the solution $\Delta_k = 0 \; \forall \; k$, which describes the normal ground state or filled Fermi sea, as can easily be verified. In addition, the gap equation also has nontrivial solutions, known as *superconducting solutions*, with $\Delta_k \neq 0$. In order to solve Eq. (2.28) for nonzero Δ_k a model interaction in D dimensions, of the form

$$\begin{aligned} V_{k,k'} &= \frac{v_0}{L^D}\,, \qquad \max(0,\, E_F - \hbar\omega_D) < \epsilon_k,\, \epsilon_{k'} < E_F + \hbar\omega_D\,, \\ &= 0 \qquad \text{otherwise}\,. \end{aligned} \tag{2.29}$$

is assumed. Here, L is the system size, the coupling strength $v_0 > 0$ signifies net *attraction* between electrons, $\hbar\omega_D$ is the maximum (Debye) energy of a phonon absorbed (or emitted) by an electron, and $E_F = \frac{\hbar^2 k_F^2}{2m^*}$ is the Fermi energy. The latter is fixed by the electron density ρ in D dimensions (see Table 2.1). In proposing this interaction, Bardeen *et al.* argued that the interaction can only affect electrons in the vicinity of the Fermi surface, since the Pauli principle prevents electrons deep inside the Fermi sphere from scattering into other states, a similar argument to the one by Cooper. It is easily verified that the BCS model interaction reduces the gap function to

$$\Delta_k = \Delta\theta(\hbar\omega_D - \mid \xi_k \mid)\,, \tag{2.30}$$

with $\theta(x)$ the Heaviside step function, and where Δ is given by the solution

D	ρ	$N(0)$
1	$\frac{2k_F}{\pi}$	$\frac{1}{\pi\hbar}\sqrt{\frac{m^*}{2E_F}}$
2	$\frac{k_F^2}{2\pi}$	$\frac{m^*}{2\pi\hbar^2}$
3	$\frac{k_F^3}{3\pi^2}$	$\frac{1}{\pi^2\hbar^3}\sqrt{\frac{m^{*3}E_F}{2}}$

Table 2.1: The electron density ρ and the density of states $N(0)$ per spin state per unit L^D, at the Fermi energy $E_F = \frac{\hbar^2 k_F^2}{2m}$, as a function of the dimensionality of the system, D.

to the gap equation (2.28) which now becomes

$$1 = \frac{v_0}{2L^D} \sum_{\mathbf{k}} \frac{\theta(\hbar\omega_D - \mid \xi_k \mid)}{\sqrt{\Delta^2 + \xi_k^2}} \,. \tag{2.31}$$

Making use of the usual prescription

$$\sum_{\mathbf{k}} \rightarrow \left(\frac{L}{2\pi}\right)^D \int d^D k \tag{2.32}$$

to convert the sum (2.31) to an integral, one obtains

$$1 = \frac{v_0}{2(2\pi)^D} \int d^D k \frac{\theta(\hbar\omega_D - \mid \xi_k \mid)}{\sqrt{\Delta^2 + \xi_k^2}} \,. \tag{2.33}$$

We define

$$\xi \;=\; \epsilon_k - \mu \;=\; \frac{\hbar^2 k^2}{2m^*} - \mu \tag{2.34}$$

so that

$$(2\pi)^{-D}\, d^D k \;=\; C_D\; (\xi + \mu)^{\frac{D-2}{2}}\; d\xi \;=\; N_D(\xi)\; d\xi \,, \tag{2.35}$$

with

$$\begin{aligned} C_1 &= \frac{1}{\pi\hbar}\sqrt{\frac{m^*}{2}} \\ C_2 &= \frac{m^*}{2\pi\hbar^2} \\ C_3 &= \frac{1}{\pi^2\hbar^3}\sqrt{\frac{m^{*3}}{2}} \,, \end{aligned} \tag{2.36}$$

and $N_D(\xi)$ is the density of states per spin state in D dimensions. Note that in two dimensions, $N_2(\xi)$ is a constant, independent of ξ. Equation (2.33) now becomes

$$1 = \frac{v_0}{2} \int d\xi\; N_D(\xi)\; \frac{\theta(\hbar\omega_D - \mid \xi \mid)}{\sqrt{\Delta^2 + \xi^2}} \,. \tag{2.37}$$

In general, the gap Δ and chemical potential μ must be found by simultaneously solving equation (2.37) and the number equation

$$N \;=\; < \Phi | \hat{N} | \Phi >$$

$$
\begin{aligned}
&= \sum_{\mathbf{k}\lambda} < \Phi | a^{\dagger}_{\mathbf{k}\lambda} a_{\mathbf{k}\lambda} | \Phi > \\
&= 2 \sum_{\mathbf{k}} v_k^2 \\
&= \sum_{\mathbf{k}} \left(1 - \frac{\xi_k}{\sqrt{\xi_k^2 + \Delta_k^2}} \right) \\
&= \left(\frac{L}{2\pi} \right)^D \int d^D k \left(1 - \frac{\xi_k}{\sqrt{\xi_k^2 + \Delta_k^2}} \right) \ . \qquad (2.38)
\end{aligned}
$$

However, in the weak coupling limit

$$\delta \equiv \frac{\Delta}{E_F} \ll 1 \ , \qquad (2.39)$$

Δ_k can be neglected in the number equation (2.38) which, with the use of Table 2.1, implies that

$$\mu \approx E_F \ . \qquad (2.40)$$

Therefore the number constraint can be taken into account by replacing the chemical potential μ by the Fermi energy E_F throughout.

For real superconductors, the BCS gap equation now has to be solved in $D = 3$ dimensions. However, since in metallic superconductors the width of the interaction in units of the Fermi energy is very small, i.e.

$$\nu \equiv \frac{\hbar\omega_D}{E_F} \ll 1 \ , \qquad (2.41)$$

one may assume the electronic density of states per spin state $N(\xi)$ to be constant at the Fermi-level value $N(0)$ (see Table 2.1) in the thin region about the Fermi surface where the interaction is nonzero. Thus, independent of the number of dimensions D, the solution of the gap equation can effectively be reduced to a *two*-dimensional problem, and Eq. (2.37) becomes

$$
\begin{aligned}
1 &= \frac{v_0 N(0)}{2} \int_{-\hbar\omega_D}^{\hbar\omega_D} \frac{d\xi}{\sqrt{\Delta^2 + \xi^2}} \\
&\approx v_0 N(0) \ln \frac{2\hbar\omega_D}{\Delta} \qquad (2.42)
\end{aligned}
$$

in the weak coupling limit where $\Delta \ll \hbar\omega_D$. Upon inverting this relation one obtains an analytic solution for the BCS gap (in units of the Fermi energy)

$$\delta \equiv \frac{\Delta}{E_F} = 2\nu \exp\left(-\frac{1}{\lambda}\right) \qquad (\lambda \to 0) \; . \tag{2.43}$$

The factor λ is dimensionless and has the form

$$\lambda \equiv v_0 N(0) \; , \tag{2.44}$$

with $N(0)$ given in Table 2.1. For reference purposes, the Cooper pair binding energy [29] in the limit $\nu \ll 1$ is also given here :

$$\delta_C \equiv \frac{\Delta_C}{E_F} = 2\nu \exp\left(-\frac{2}{\lambda}\right) \qquad (\lambda \to 0) \; . \tag{2.45}$$

It remains to be shown that, in the BCS model, the superconducting solution has a lower ground state energy E_s^0 than the normal ground state energy E_n^0. This calculation is readily performed in the weak coupling limit, and one finds [31]

$$E_s^0 - E_n^0 \; = \; -\frac{1}{2} N(0) L^D \Delta^2 \; . \tag{2.46}$$

This expression corresponds to the binding energy Δ per pair multiplied by the number of pairs $\frac{1}{2}N(0)L^D\Delta$ lying within a "shell" of thickness Δ around the Fermi surface, since these are the pairs that can lower their energy by forming a Cooper pair bound state. It is clear that the superconducting solution yields an energetically favourable ground state. The gain in kinetic energy due to the occupation of states above the normal Fermi level is outweighed by the binding energy of the Cooper pairs.

Consider now the simplest exited state, namely the "broken pair" state in which one member of the pair $(\mathbf{k}, -\mathbf{k})$ is occupied and the other is unoccupied. Denote the energy of this state by E_s^1. The transition from E_s^0 to E_s^1 is accompanied by a gain in energy due to the kinetic energy of the newly occupied state, and a loss in energy due to the loss of the binding energy of the pair. Using Eqs. (2.19) and (2.23) we may write

$$\begin{aligned} E_s^1 - E_s^0 \; &= \; \xi_k \; - \; 2\xi_k v_k^2 + 2\Delta_k u_k v_k \\ &= \; \xi_k \; - \; \xi_k \left(1 - \frac{\xi_k}{E_k}\right) \; + \; \frac{\Delta_k^2}{E_k} \\ &= \; \frac{\xi_k^2 + \Delta_k^2}{E_k} \; = \; E_k \; , \end{aligned} \tag{2.47}$$

where (2.26), (2.27) and (2.28) have been used. Thus E_k is the energy of an *elementary excitation* or *quasiparticle*. But in the BCS model

$$E_k \geq \Delta \quad \forall\, \mathbf{k}\,, \tag{2.48}$$

which clearly indicates a gap Δ in the excitation spectrum of the superconducting state. That is, all excited states have energy at least Δ above the ground state energy E_s^0. The fact that this basic property of metallic superconductors flows naturally from BCS theory, is a tribute to the physical insight of its originators.

2.3 Finite temperature BCS theory

At zero temperature the BCS state is described by the single wave function $|\Phi>$ of Eq. (2.5). At nonzero temperature higher-lying states become accessible due to thermal excitations, and one must deal with a statistical ensemble. Introduce the notation $|10>$ to denote the state where the first element of the pair $(\mathbf{k},\uparrow),(-\mathbf{k},\downarrow)$ is occupied, and the other is unoccupied. Then the symbols $|00>$, $|01>$ and $|11>$ have the obvious meaning. In the BCS ground state at $T=0$ only the occupation of the states $|00>$ and $|11>$ was considered. At finite temperature we introduce f_k, the probability that the states $|01>$ or $|10>$ are occupied. Then $1-2f_k$ is the probability that the states considered in $|\Phi>$ are occupied.

We now minimize the thermodynamic potential Ω defined by

$$\Omega \;=\; \left\langle \hat{K} \right\rangle - T\Sigma\,, \tag{2.49}$$

where $\left\langle \hat{K} \right\rangle$ is an ensemble average, and Σ denotes the entropy. The kinetic term is simply

$$\left\langle \hat{K}_{kin} \right\rangle \;=\; \sum_{\mathbf{k}} \left[2f_k\xi_k \;+\; 2\left(1-2f_k\right) v_k^2 \xi_k \right]\,, \tag{2.50}$$

and the ensemble average of the potential is given by

$$\left\langle \hat{K}_{pot} \right\rangle \;=\; \sum_{\mathbf{k},\mathbf{k}'} V_{\mathbf{k}\mathbf{k}'} u_k v_k u_{k'} v_{k'} \left(1-2f_k\right)\left(1-2f_{k'}\right)\,, \tag{2.51}$$

since the interaction only occurs when the states considered in $|\Phi>$ are occupied. Following the discussion in the previous section on the BCS excited states at $T = 0$, we assume that the states described by f_k are single-particle-like. This allows one to use the standard expression for the entropy of a Fermi-Dirac gas, *viz.*

$$\Sigma \;=\; -2k_B \sum_{\mathbf{k}} \left[f_k \ln f_k \;+\; (1 - f_k) \ln (1 - f_k) \right] \;, \tag{2.52}$$

where k_B is Boltzmann's constant.

Equations (2.49) - (2.52) now give an explicit form for the thermodynamic potential Ω in terms of the variational parameters v_k and f_k. Since the entropy Σ is independent of v_k, the minimization of Ω with respect to v_k goes through analogous to the zero temperature case, provided that the temperature dependent BCS gap Δ_k is defined as

$$\Delta_k \;\equiv\; \sum_{\mathbf{k}'} V_{\mathbf{k}\mathbf{k}'} u_{k'} v_{k'} \left(1 - 2 f_{k'} \right) \;. \tag{2.53}$$

With this definition, it is easily shown that the finite temperature BCS gap equation is given by

$$\Delta_k \;=\; \sum_{\mathbf{k}'} V_{\mathbf{k}\mathbf{k}'} \frac{\Delta_{k'}}{2E_{k'}} \left(1 - 2 f_{k'} \right) \;. \tag{2.54}$$

The explicit form of f_k is found by minimizing Ω with respect to f_k, and one obtains

$$\frac{\partial \Omega}{\partial f_k} \;=\; 2\xi_k \left(1 - 2v_k^2 \right) \;-\; 4 u_k v_k \Delta_k \;+\; 2k_B T \ln \left[\frac{f_k}{1 - f_k} \right] \;=\; 0 \;, \tag{2.55}$$

where the definition (2.53) has been used. In terms of the angle χ_k introduced in (2.24) this becomes

$$\xi_k \cos 2\chi_k \;+\; \Delta_k \sin 2\chi_k \;+\; k_B T \ln \left[\frac{f_k}{1 - f_k} \right] \;=\; 0 \;, \tag{2.56}$$

which, with the use of Eqs. (2.26) and (2.27), reduces to

$$E_k \;+\; k_B T \ln \left[\frac{f_k}{1 - f_k} \right] \;=\; 0 \;, \tag{2.57}$$

so that

$$f_k = \frac{1}{1+\exp\frac{E_k}{k_BT}} . \tag{2.58}$$

This clearly has the form of a Fermi-Dirac distribution for the energy E_k, which vindicates our interpretation of E_k as the energy of a fermion quasi-particle excitation, and the use of (2.52) for the entropy. Just as at zero temperature, Δ_k is the energy gap for excitations, but now the gap is temperature dependent via the thermal occupation probability f_k. This temperature dependence is obtained by substituting Eq. (2.58) into the previous expression (2.54) for the energy gap, and one finds

$$\Delta_k = \sum_{\mathbf{k}'} V_{\mathbf{k}\mathbf{k}'} \frac{\Delta_{k'}}{2E_{k'}} \tanh \frac{E_{k'}}{2k_BT} . \tag{2.59}$$

For the BCS model interaction (2.29) in D dimensions, this becomes

$$1 = \frac{v_0}{2L^D} \sum_{\mathbf{k}} \frac{\theta(\hbar\omega_D - \mid \xi_k \mid)}{\sqrt{\Delta^2+\xi_k^2}} \tanh \frac{\sqrt{\Delta^2+\xi_k^2}}{2k_BT} , \tag{2.60}$$

which, in three dimensions, may be converted to an integral using (2.32) as before, to obtain

$$1 = \lambda \int_0^{\hbar\omega_D} \frac{d\xi}{\sqrt{\Delta^2+\xi^2}} \tanh \frac{\sqrt{\Delta^2+\xi^2}}{2k_BT} , \tag{2.61}$$

with $\lambda = v_0 N(0)$ as before. It is clear that this equation reduces to the zero temperature result (2.42) in the limit $T \to 0$. Equation (2.61) cannot be solved analytically, but since the gap tends to zero when T approaches the critical temperature T_c, it yields an implicit equation for T_c when we set $\Delta = 0$:

$$1 = \lambda \int_0^{\hbar\omega_D} \frac{d\xi}{\xi} \tanh \frac{\xi}{2k_BT_c} . \tag{2.62}$$

In the weak coupling limit $\lambda \ll 1$, this gives [31]

$$k_BT_c = 1.13\hbar\omega_D \exp\left(-\frac{1}{\lambda}\right) . \tag{2.63}$$

Equation (2.63) explains the isotope effect. Since $\omega_D \propto \left(\frac{K}{M}\right)^{\frac{1}{2}}$, with K the force constant of the lattice and M the ionic mass, it follows that $T_c \propto M^{-\frac{1}{2}}$. Furthermore, since (2.63) contains the same exponential factor as the zero temperature BCS gap $\Delta(0)$, the ratio

$$\frac{2\Delta(0)}{k_B T_c} = 3.52 \tag{2.64}$$

is a universal constant independent of the particular material. These predictions are satisfied reasonably well in practice by metallic superconductors [31, 3]. Deviations occur due to the simplistic nature of the BCS model interaction, and the implicit assumption of a spherical Fermi surface, which need not hold in a real superconductor. Known thermodynamic properties of metallic superconductors such as the exponentially decaying specific heat at low temperatures, and electrodynamic properties such as the behaviour of the critical magnetic field and the exclusion of magnetic flux via the Meissner effect [32], can also be shown to follow from BCS theory [31]. Thus the theory provides a very good description and understanding of metallic superconductivity.

Typically the maximum values for $\frac{\hbar\omega_D}{k_B}$ and λ are in the order of 400 and 0.4, respectively. Substituting these values into Eq. (2.63), one obtains

$$T_c \approx 40K \ , \tag{2.65}$$

which gives an upper bound for the transition temperature in the phononic BCS model. This so called "phonon barrier" prevents conventional BCS theory from providing an adequate description of the new high T_c superconductors. However, it is clear that this is only true if one assumes that the electron-electron interaction responsible for pairing is phonon mediated. This need not necessarily be the case, and provides the motivation for the work done in the following chapter.

Chapter 3

Analytic Solution of the BCS Gap Equation

3.1 Dimensionality considerations

As described in Chapter 2 the BCS model interaction (2.29) is introduced in conventional low-temperature superconductivity to mimic the net electron-electron interaction responsible for electron pairing in three dimensions. Since in metallic superconductors the width of the interaction in units of the Fermi energy is small, i.e.

$$\nu = \frac{\hbar\omega_D}{E_F} \ll 1 \,, \tag{3.1}$$

the solution of the BCS gap equation effectively becomes a *two*-dimensional problem.

Although phonon-mediated superconductivity cannot describe exotic (including high-temperature) superconductors, a BCS-like theory in which the mediating bosons are *not* phonons may still apply. It could therefore be useful to solve the BCS gap equation in one, two, and three dimensions, again for weak coupling, but *without* the restriction (3.1). It is appropriate to do so since exotic superconductors can be quasi-1D (organics), quasi-2D (organics, cuprates), and 3D (bismuthates, heavy-fermion metals, Chevrel-phases, fullerides). This calculation can be viewed as a preliminary step towards the more extensive revision of the standard BCS model which will be necessary if a BCS-like theory is to describe exotic superconductors [17].

Furthermore, it is known that 2D quantum binding in a well exhibits an essential singularity in coupling (not present in one or three dimensions), similar to that observed in the expressions for the BCS gap (2.43) and the Cooper energy gap (2.45), in the limit $\nu \ll 1$. This makes it tempting to attribute the singularity in the Cooper *and* BCS results to a dimensionality effect. However, it has been shown recently [33, 34] that the Cooper pair binding energy exhibits the same essential singularity in the coupling constant in one, two and three dimensions, regardless of the interaction width ν. We now show that, independent of the value of ν, the BCS gap parameter can be written in the universal form

$$\delta \equiv \frac{\Delta}{E_F} = f_D(\nu) \exp\left(-\frac{1}{\lambda}\right), \tag{3.2}$$

where the analytical dimension-dependent functions $f_D(\nu)$ are given in Table 3.1 [19, 20], and

$$\lambda = v_0 N(0) \tag{3.3}$$

as before. Table 3.1 indicates clearly that the essential singularity in coupling persists, and cannot be ascribed to the quasi-two-dimensional nature of phononic superconductivity implied by the limit $\nu \ll 1$.

D	$f_D(\nu) \quad \nu \leq 1$	$f_D(\nu) \quad \nu > 1$
1	$\frac{8}{\nu}\left(\sqrt{1+\nu}-1\right)\left(1-\sqrt{1-\nu}\right)$	$\frac{8}{\sqrt{\nu}}\left(\sqrt{1+\nu}-1\right)$
2	2ν	$2\sqrt{\nu}$
3	$\frac{8}{\nu}\left(\sqrt{1+\nu}-1\right)\left(1-\sqrt{1-\nu}\right)e^{\sqrt{1+\nu}+\sqrt{1-\nu}-2}$	$\frac{8}{\sqrt{\nu}}\left(\sqrt{1+\nu}-1\right)e^{\sqrt{1+\nu}-2}$

Table 3.1: The expressions $f_D(\nu)$ which give the analytic form for the BCS gap (3.2), as a function of the dimensionality of the system, D.

3.2 Some results from quantum binding in a well

The ground state energy of an attractive, rectangular 1D well of depth V_0 and range a can be expanded about small V_0a^2 in the following manner [33]:

$$E \overset{V_0a^2\to 0}{\longrightarrow} -\frac{2ma^2V_0^2}{\hbar^2} + O(V_0^3) \qquad (1D) \tag{3.4}$$

Similarly, in the case of a spherical 3D-well of depth V_0 and radius a, an expansion for the ground state energy about small $\eta \equiv V_0a^2 - \frac{\hbar^2\pi^2}{8m}$ gives

$$E \overset{\eta\to 0}{\longrightarrow} -\frac{m\eta^2}{2\hbar^2\pi^2} + O(\eta^3) \qquad (3D)\,. \tag{3.5}$$

These are both *perturbative* expansions in an appropriate "smallness" parameter. The 2D-case, however, is non-perturbative and gives

$$E \overset{V_0a^2\to 0}{\longrightarrow} -\frac{\hbar^2}{2ma^2}\exp\left(-\frac{2\hbar}{mV_0a^2}\right) \qquad (2D) \tag{3.6}$$

which has the same singularity structure in coupling as the Cooper pair binding energy (2.45), and the BCS gap (2.43).

3.3 Analytic solution for the BCS gap in D dimensions

Since the single-particle energies ϵ_k must be non-negative, two cases must be distinguished:
a) If $\nu \equiv \frac{\hbar\omega_D}{E_F} \leq 1$, the energy integration region is symmetric, namely it is given by

$$E_F - \hbar\omega_D \leq \epsilon_k \leq E_F + \hbar\omega_D\,. \tag{3.7}$$

b) If $\nu > 1$, the energy integration region becomes asymmetric, and is given by

$$0 \leq \epsilon_k \leq E_F + \hbar\omega_D\,. \tag{3.8}$$

Subject to this constraint, the BCS gap equation (2.42) is now solved analytically in one, two, and three dimensions. Converting equation (2.42) to an integral over energy, one obtains

$$1 = \frac{\lambda}{2} \int_{E_F - \hbar\omega_D, 0}^{E_F + \hbar\omega_D} \frac{\left(\frac{\epsilon}{E_F}\right)^{\frac{D-2}{2}} d\epsilon}{\sqrt{\Delta^2 + (\epsilon - E_F)^2}} , \tag{3.9}$$

where (2.44) has been used. This integral may be split up into two parts,

$$\begin{aligned} \frac{2}{\lambda} &= \int_{1-\nu,0}^{1+\nu} \frac{d\epsilon}{\sqrt{\delta^2 + (\epsilon - 1)^2}} + \int_{1-\nu,0}^{1+\nu} \frac{\epsilon^{\left(\frac{D-2}{2}\right)} - 1}{\sqrt{\delta^2 + (\epsilon - 1)^2}} d\epsilon \\ &= I + I_D , \end{aligned} \tag{3.10}$$

which defines I and I_D, and where the energy has been expressed in units of E_F for convenience. In both integrals the lower limit refers to (3.7) or (3.8), and $\delta \equiv \frac{\Delta}{E_F}$ as before.

The integral I is independent of the number of dimensions, D, and is easily evaluated to give

$$\begin{aligned} I &= 2 \ln\left(\frac{2\nu}{\delta}\right) \qquad \text{if } \nu \leq 1 \\ &= 2 \ln\left(\frac{2\sqrt{\nu}}{\delta}\right) \qquad \text{if } \nu > 1 . \end{aligned} \tag{3.11}$$

Since the integral I_D is finite for $\delta = 0$, the δ dependence in I_D may be neglected if $\delta \ll 1$, and one obtains

$$I_D = \int_{1-\nu,0}^{1+\nu} \frac{\epsilon^{\left(\frac{D-2}{2}\right)} - 1}{\mid \epsilon - 1 \mid} d\epsilon , \tag{3.12}$$

which upon integration gives

$$\begin{aligned} I_D &= 2 \ln\left[\frac{4}{\left(1 + \sqrt{1-\nu}\right)\left(1 + \sqrt{1+\nu}\right)}\right] && (D = 1) \\ &= 0 && (D = 2) \\ &= 2 \ln\left[\frac{4}{\left(1 + \sqrt{1-\nu}\right)\left(1 + \sqrt{1+\nu}\right)}\right] + 2\sqrt{1+\nu} + 2\sqrt{1-\nu} - 4 \\ & && (D = 3) . \end{aligned} \tag{3.13}$$

In arriving at the results (3.13) it has implicitly been assumed that $\nu \leq 1$. If $\nu > 1$, it is easily shown that one simply replaces the factor $(1-\nu)$ in the above expressions by 0. Equations (3.11) and (3.13) may be substituted into (3.10), which upon inversion gives

$$\delta = f_D(\nu) \exp\left(-\frac{1}{\lambda}\right) , \tag{3.14}$$

where the dimension-dependent functions $f_D(\nu)$ are given in Table 3.1.

For a thin shell about the Fermi surface, i.e. $\nu \ll 1$, one obtains

$$\begin{aligned} f_D(\nu) &= 2\nu\left(1+\frac{3\nu^2}{16}\right) + O(\nu^5) && (D=1) \\ &= 2\nu && (D=2) \\ &= 2\nu\left(1-\frac{\nu^2}{16}\right) + O(\nu^5) && (D=3) , \end{aligned} \tag{3.15}$$

which give the lowest order corrections to the BCS result (2.43). For conventional metallic superconductors, $\nu = \frac{\hbar\omega_D}{E_F}$ is of order 10^{-3}, and hence the corrections in one and three dimensions are entirely negligible, since they are of order 10^{-7}. For these corrections to have a 5 % effect on the gap parameter, the interaction width would have to be of order 10^{-1}.

If the width of the interaction is equal to the Fermi energy, i.e. $\nu = 1$, the functions $f_D(\nu)$ become

$$\begin{aligned} f_D(\nu) &= 8\left(\sqrt{2}-1\right) \approx 3.31 && (D=1) \\ &= 2 && (D=2) \\ &= 8\left(\sqrt{2}-1\right) e^{\sqrt{2}-2} \approx 1.84 && (D=3) . \end{aligned} \tag{3.16}$$

Finally, for $\nu \gg 1$ the gap δ tends towards a finite limit in one dimension [35], but diverges in two and three dimensions. This limit, however, corresponds to an attractive delta pair potential in coordinate space, which is known to produce a collapsed ground state energy for a many-fermion system in two or three dimensions.

3.4 Conclusions

Analytic expressions for the BCS gap parameter $\Delta \equiv \delta E_F$ in the form

$$\delta = f_D(\nu) \exp\left(-\frac{1}{\lambda}\right) \tag{3.17}$$

were obtained in the weak coupling ($\lambda \ll 1$) limit in one, two and three dimensions for an arbitrary width, $\nu \equiv \frac{\hbar\omega_D}{E_F}$, of the BCS model interaction, with the functions $f_D(\nu)$ given in Table 3.1. It should be mentioned here that the results of this table have previously been published by Eagles [19]. Unfortunately, as there is no mention of these results in the abstract of the article [19], my supervisor and I only became aware of this fact after our article, in collaboration with M de Llano, on this subject [20] had already been accepted for publication.

We conclude that the essential singularity in coupling in the BCS gap does not arise from the two-dimensional character of the BCS model interaction in the case $\nu \ll 1$, but is rather an intrinsic feature of the model, at least in the weak coupling limit.

Chapter 4

The Functional Integral Representation of the Partition Function

In the finite temperature BCS formalism, a form is assumed for the ground state and the quasiparticle excitation spectrum of a system. The free energy F of the system is determined as an ensemble average for a given inverse temperature $\beta = \frac{1}{k_B T}$, and F is then minimized to obtain the most probable configuration of the system. This is essentially a mean-field approach, which neglects statistical fluctuations of the system into states other than the most probable state, due to thermal excitations.

Fluctuations also arise because the system is assumed to be in a state which is not necessarily an exact eigenstate of the system. In a BCS framework, these so called quantum fluctuations occur, for instance, due to the fact that BCS ground state violates particle number symmetry. Furthermore, there is no guarantee that quasiparticle excitation as described in section 2.3 is the only means of excitation available to the system.

At low temperatures, thermal excitations may be neglected, and for large systems in the thermodynamic limit, the fluctuations in particle number are also negligible. However, for finite systems at nonzero temperature, these fluctuations can have a significant effect, and must be taken into account. The individual grains of polycrystalline high-T_c superconductors fall into this category. Since these grains are usually weakly coupled, they may as a first approximation be treated as isolated systems [24]. The effect of finite system

size should be even more pronounced in nuclei that undergo a BCS-type pairing transition, since here the number of nucleons is not only finite but small.

The fluctuations described above can be incorporated into our calculations via a functional integral representation of the grand partition function. This representation may be evaluated using various approximation schemes to include the effect of certain fluctuations. The next section contains a formal derivation of the functional integral (also known as the path integral) representation of the partition function, developed by Hubbard [36] and Stratonovich [37]. In section 4.2 the static path approximation (SPA) [38] is reviewed. In section 4.3, the functional integral representation of the partition function is compared with the Landau order parameter representation, in order to examine the physical content of the SPA. This comparison also suggests an appropriate choice for the "order parameter" in a pairing system, as discussed in section 4.4. Finally, section 4.5 deals with the RPA-SPA approximation [39, 40] of Puddu *et al.* to the grand partition function, which includes some of the quantum fluctuations.

4.1 The functional integral method

The partition function in the grand canonical ensemble is given by

$$\mathcal{Z}(\beta,\alpha) \;=\; \mathrm{Tr}\left[e^{-\beta H+\alpha N}\right] \;. \tag{4.1}$$

Here the inverse temperature parameters $\beta = (k_B T)^{-1}$ and $\alpha = \beta\mu$, with μ the chemical potential, are fixed by the energy and particle number of the system by the conditions

$$\begin{aligned} E &= -\frac{\partial \ln \mathcal{Z}}{\partial \beta} \\ N &= \frac{\partial \ln \mathcal{Z}}{\partial \alpha} \;. \end{aligned} \tag{4.2}$$

Given the modified BCS-like pairing Hamiltonian [2]

$$\begin{aligned} K &= H - \mu N \\ &= \sum_k (\epsilon_k - \mu)\left(a_k^\dagger a_k + a_{\overline{k}}^\dagger a_{\overline{k}}\right) \;-\; G\sum_{k,k'} a_k^\dagger a_{\overline{k}}^\dagger a_{\overline{k'}} a_{k'} \;, \end{aligned} \tag{4.3}$$

where k and $\overline{k}$ denote the states forming a pair, e.g. $(k,\uparrow)$ and $(-k,\downarrow)$, one may define the pairing operator

$$P = \sum_k a_{\overline{k}} a_k \,, \tag{4.4}$$

and perform the transformation

$$\begin{aligned} X &= \frac{1}{2}\left(P + P^\dagger\right) \\ Y &= \frac{i}{2}\left(P - P^\dagger\right) \,. \end{aligned} \tag{4.5}$$

The modified Hamiltonian is now given in terms of the operators X and Y as

$$K = K_0 - G\left(X^2 + Y^2\right) \,, \tag{4.6}$$

with

$$K_0 = \sum_k \left[\epsilon_k - \mu + \left(\epsilon_k - \mu - \frac{G}{2}\right)\left(a_k^\dagger a_k + a_{\overline{k}}^\dagger a_{\overline{k}} - 1\right)\right] \,. \tag{4.7}$$

This form is then quadratic in the operators X and Y, and therefore quartic in the fermion operators. Thus we may apply the Hubbard-Stratonovich transformation [36, 37] to obtain an exact path integral representation, linear in X and Y, for the grand partition function. In order to achieve this linearization, it would be convenient to make use of the identity

$$e^{-\beta(A-\gamma B^2)} = \left(\frac{\beta\gamma}{\pi}\right)^{\frac{1}{2}} \int_{-\infty}^{\infty} dx \; e^{-\beta\gamma x^2} e^{-\beta(A-2\gamma x B)} \,. \tag{4.8}$$

This identity is unfortunately only valid for operators A and B that commute, and this is not the case for K_0 and either X or Y. Nevertheless, it is still possible to make use of Eq. (4.8). To this end, let us consider the inverse temperature β as an imaginary time, and divide the interval $(0,\beta)$ into M intervals of length Δt so that

$$\beta = M\Delta t \,, \tag{4.9}$$

and further define $t_n \equiv n\Delta t$. We now introduce a fictitious "time dependence" into the operators K_0, X and Y, which will permit one to apply

Eq. (4.8). In the limit $\Delta t \to 0$, or equivalently $M \to \infty$, we may then write [41]

$$\begin{aligned} e^{-\beta K} &= \tau\, e^{-\sum_{n=1}^{M} \Delta t\, K(t_n)} = \tau\, e^{-\frac{\beta}{M}\sum_{n=1}^{M} K(t_n)} \\ &= \tau \prod_{n=1}^{M} e^{-\frac{\beta}{M}\left[K_0(t_n) - G\left\{X^2(t_n)+Y^2(t_n)\right\}\right]} . \end{aligned} \tag{4.10}$$

Here we have introduced the imaginary time ordering operator τ, which allows one to treat the operators $K_0(t_n)$, $X(t_n)$ and $Y(t_n)$ as c numbers, with the definition

$$\tau\, K_0(t_i)X(t_j) = \tau\, X(t_j)K_0(t_i) = \begin{cases} K_0X & \text{for} \quad t_i > t_j \\ XK_0 & \text{for} \quad t_j > t_i \end{cases} , \tag{4.11}$$

and similarly for K_0 and Y. If $t_i = t_j$, then t_j is interpreted as a time infinitesimally later than t_i. Thus K_0, X and Y are treated as though they are "time dependent" operators which commute at different "times". Applying Eq. (4.8) to the n th term in the product (4.10), for both $X(t_n)$ and $Y(t_n)$, we obtain

$$\begin{aligned} e^{-\frac{\beta}{M}\left[K_0(t_n) - G\left\{X^2(t_n)+Y^2(t_n)\right\}\right]} &= \lim_{M\to\infty}\left(\frac{\beta G}{\pi M}\right) \int d\phi_x(t_n) d\phi_y(t_n) e^{-\frac{\beta G}{M}\left\{\phi_x^2(t_n)+\phi_y^2(t_n)\right\}} \\ &\quad \times \tau\left[e^{-\frac{\beta}{M}\left\{K_0(t_n) - 2G\left[X(t_n)\phi_x(t_n)+Y(t_n)\phi_y(t_n)\right]\right\}}\right] \end{aligned} \tag{4.12}$$

Substituting (4.6) into (4.1), and applying the above procedure for all n, we obtain an exact path integral representation for the grand partition function [41, 40]

$$\begin{aligned} \mathcal{Z} = \lim_{M\to\infty}\left(\frac{\beta G}{\pi M}\right)^M \int \prod_{n=1}^{M} d\phi_x(t_n) d\phi_y(t_n) \Big\{ & e^{-\frac{\beta G}{M}\sum_{n=1}^{M} \phi_x^2(t_n)+\phi_y^2(t_n)} \\ & \times \mathrm{Tr}\left[\tau e^{-\frac{\beta}{M}\sum_{n=1}^{M} \mathcal{K}_n(t_n)}\right]\Big\} , \end{aligned} \tag{4.13}$$

with

$$\mathcal{K}_n(t_n) = K_0(t_n) - 2G\left[X(t_n)\phi_x(t_n) + Y(t_n)\phi_y(t_n)\right] . \tag{4.14}$$

Note here that the trace operation ensures that $\phi_x(0) = \phi_x(t_M) = \phi_x(\beta)$ and similarly for $\phi_y(t_n)$.

4.2 The SPA approximation to the grand partition function

In order to define the various approximation schemes, it is convenient to work with the Fourier series expansion of the periodic fields $\phi_x(t)$ and $\phi_x(t)$ in equation (4.13). Assume that we have chosen an odd number M of "time" slices. Then

$$\phi_x(t) \;=\; \overline{\eta}_x \;+ \sum_{p=-\frac{M-1}{2},\, p\neq 0}^{\frac{M-1}{2}} \eta_{xp} e^{-i\frac{2\pi p}{\beta}t} \,. \tag{4.15}$$

Here η_{xp} is a complex variable with $\eta^*_{xp} = \eta_{x-p}$ to ensure that $\phi_x(t)$ is real. It is easily shown that $\overline{\eta}_x = \eta_{x0}$ represents the "time" average of the field $\phi_x(t)$ over the interval $(0,\beta)$. Similar relations hold for $\phi_y(t)$. In the static path approximation (SPA) [38], one considers only the contributions of $\overline{\eta}_x$ and $\overline{\eta}_y$ to the trace in Eq. (4.13), so that $\mathcal{K}_n(t_n)$ is replaced by its "time" average

$$\overline{\mathcal{K}} \;=\; K_0 \;-\; 2G(X\overline{\eta}_x + Y\overline{\eta}_y) \,. \tag{4.16}$$

Furthermore, one may convert the sum over time slices to an integral to obtain

$$\begin{aligned}\lim_{M\to\infty} \frac{\beta G}{M} \sum_{n=1}^{M} \left\{\phi_x^2(t_n) \;+\; \phi_y^2(t_n)\right\} \;&=\; G\int_0^\beta dt\, \left\{\phi_x^2(t) \;+\; \phi_y^2(t)\right\} \\ &=\; \beta G \left\{ \overline{\eta}_x^2 \;+\; \overline{\eta}_y^2 + 2\sum_{p=1}^{\frac{M-1}{2}} \left[|\eta_{xp}|^2 + |\eta_{yp}|^2\right] \right\} \end{aligned} \tag{4.17}$$

which yields for the grand partition function

$$\begin{aligned}\mathcal{Z}_{SPA} \;=\; &\lim_{M\to\infty} \left(\frac{\beta G}{\pi M}\right)^M \int \mathcal{J}\left(\frac{\phi_x(t_n)}{\eta_{xp}}\right) \mathcal{J}\left(\frac{\phi_y(t_n)}{\eta_{yp}}\right) \prod_{p=1}^{\frac{M-1}{2}} d\eta_{xp} d\eta^*_{xp} d\eta_{yp} d\eta^*_{yp} \;\times \\ &e^{-2\beta G\sum_{p=1}^{\frac{M-1}{2}} \{|\eta_{xp}|^2 + |\eta_{yp}|^2\}} \int d\overline{\eta}_x d\overline{\eta}_y \left\{ e^{-\beta G\left(\overline{\eta}_x^2 + \overline{\eta}_y^2\right)} \,\mathrm{Tr}\left[e^{-\beta\overline{\mathcal{K}}}\right]\right\} \,. \end{aligned} \tag{4.18}$$

Here the Jacobian $\mathcal{J}\left(\frac{\phi_x(t_n)}{\eta_{xp}}\right)$ of the transformation from $\{\phi_x(t_n)\}$ to $\{\eta_{xp}\}$ is given by

$$\mathcal{J}\left(\frac{\phi_x(t_n)}{\eta_{xp}}\right) = \begin{vmatrix} \frac{\partial\phi_x(t_1)}{\partial\eta_{x0}} & \frac{\partial\phi_x(t_1)}{\partial\eta_{x1}} & \frac{\partial\phi_x(t_1)}{\partial\eta^*_{x1}} & \frac{\partial\phi_x(t_1)}{\partial\eta_{x2}} & \frac{\partial\phi_x(t_1)}{\partial\eta^*_{x2}} & \cdots & \frac{\partial\phi_x(t_1)}{\partial\eta_{x\frac{M-1}{2}}} & \frac{\partial\phi_x(t_1)}{\partial\eta^*_{x\frac{M-1}{2}}} \\ \frac{\partial\phi_x(t_2)}{\partial\eta_{x0}} & \frac{\partial\phi_x(t_2)}{\partial\eta_{x1}} & \frac{\partial\phi_x(t_2)}{\partial\eta^*_{x1}} & \frac{\partial\phi_x(t_2)}{\partial\eta_{x2}} & \frac{\partial\phi_x(t_2)}{\partial\eta^*_{x2}} & \cdots & \frac{\partial\phi_x(t_2)}{\partial\eta_{x\frac{M-1}{2}}} & \frac{\partial\phi_x(t_2)}{\partial\eta^*_{x\frac{M-1}{2}}} \\ \frac{\partial\phi_x(t_3)}{\partial\eta_{x0}} & \frac{\partial\phi_x(t_3)}{\partial\eta_{x1}} & \frac{\partial\phi_x(t_3)}{\partial\eta^*_{x1}} & \frac{\partial\phi_x(t_3)}{\partial\eta_{x2}} & \frac{\partial\phi_x(t_3)}{\partial\eta^*_{x2}} & \cdots & \frac{\partial\phi_x(t_3)}{\partial\eta_{x\frac{M-1}{2}}} & \frac{\partial\phi_x(t_3)}{\partial\eta^*_{x\frac{M-1}{2}}} \\ \vdots & \vdots & \vdots & \vdots & \vdots & & \vdots & \vdots \\ \frac{\partial\phi_x(t_M)}{\partial\eta_{x0}} & \frac{\partial\phi_x(t_M)}{\partial\eta_{x1}} & \frac{\partial\phi_x(t_M)}{\partial\eta^*_{x1}} & \frac{\partial\phi_x(t_M)}{\partial\eta_{x2}} & \frac{\partial\phi_x(t_M)}{\partial\eta^*_{x2}} & \cdots & \frac{\partial\phi_x(t_M)}{\partial\eta_{x\frac{M-1}{2}}} & \frac{\partial\phi_x(t_M)}{\partial\eta^*_{x\frac{M-1}{2}}} \end{vmatrix}$$

$$= \begin{vmatrix} 1 & e^{-i\frac{2\pi t_1}{\beta}} & e^{i\frac{2\pi t_1}{\beta}} & e^{-i\frac{4\pi t_1}{\beta}} & e^{i\frac{4\pi t_1}{\beta}} & \cdots & e^{-i\frac{(M-1)\pi t_1}{\beta}} & e^{i\frac{(M-1)\pi t_1}{\beta}} \\ 1 & e^{-i\frac{2\pi t_2}{\beta}} & e^{i\frac{2\pi t_2}{\beta}} & e^{-i\frac{4\pi t_2}{\beta}} & e^{i\frac{4\pi t_2}{\beta}} & \cdots & e^{-i\frac{(M-1)\pi t_2}{\beta}} & e^{i\frac{(M-1)\pi t_2}{\beta}} \\ 1 & e^{-i\frac{2\pi t_3}{\beta}} & e^{i\frac{2\pi t_3}{\beta}} & e^{-i\frac{4\pi t_3}{\beta}} & e^{i\frac{4\pi t_3}{\beta}} & \cdots & e^{-i\frac{(M-1)\pi t_3}{\beta}} & e^{i\frac{(M-1)\pi t_3}{\beta}} \\ \vdots & \vdots & \vdots & \vdots & \vdots & & \vdots & \vdots \\ 1 & e^{-i\frac{2\pi t_M}{\beta}} & e^{i\frac{2\pi t_M}{\beta}} & e^{-i\frac{4\pi t_M}{\beta}} & e^{i\frac{4\pi t_M}{\beta}} & \cdots & e^{-i\frac{(M-1)\pi t_M}{\beta}} & e^{i\frac{(M-1)\pi t_M}{\beta}} \end{vmatrix}$$

$$= M^{\frac{M}{2}} , \tag{4.19}$$

where the last line was obtained using a mathematical software package, and a similar result holds for $\mathcal{J}\left(\frac{\phi_y(t_n)}{\eta_{yp}}\right)$. Making the transformation

$$\begin{aligned} \eta_{xp} &= r_{xp}e^{i\theta_{xp}} \\ \eta^*_{xp} &= r_{xp}e^{-i\theta_{xp}} , \end{aligned} \tag{4.20}$$

with a similar transformation for η_{yp}, the expression (4.18) becomes

$$\begin{aligned} \mathcal{Z}_{SPA} &= \lim_{M\to\infty}\left(\frac{\beta G}{\pi}\right)^M (4\pi)^{M-1} \int \prod_{p=1}^{\frac{M-1}{2}} dr_{xp}dr_{yp}r_{xp}r_{yp}e^{-2\beta G\sum_{p=1}^{\frac{M-1}{2}}\{r^2_{xp}+r^2_{yp}\}} \\ &\quad \times \int d\overline{\eta}_x d\overline{\eta}_y \left\{e^{-\beta G\left(\overline{\eta}^2_x+\overline{\eta}^2_y\right)} \operatorname{Tr}\left[e^{-\beta\overline{\mathcal{K}}}\right]\right\} . \end{aligned} \tag{4.21}$$

The Gaussian integrals over r_{xp} and r_{yp} are now easily performed to give [40]

$$\mathcal{Z}_{SPA} = \left(\frac{\beta G}{\pi}\right) \int d\overline{\eta}_x d\overline{\eta}_y \left\{e^{-\beta G\left(\overline{\eta}^2_x+\overline{\eta}^2_y\right)} \operatorname{Tr}\left[e^{-\beta\overline{\mathcal{K}}}\right]\right\} . \tag{4.22}$$

In order to evaluate the trace, we define [25]

$$\psi \;=\; G\left(\overline{\eta}_x + i\overline{\eta}_y\right) \tag{4.23}$$

with

$$d\psi \;\equiv\; d\left(Re\;\psi\right)\; d\left(Im\;\psi\right) \;=\; G^2 d\overline{\eta}_x d\overline{\eta}_y \tag{4.24}$$

so that

$$\mathcal{Z}_{SPA} \;=\; \frac{\beta}{\pi G}\int d\psi\left\{\mathrm{Tr}\left[e^{-\beta h(\psi)}\right]\right\}\;, \tag{4.25}$$

with

$$\begin{aligned} h(\psi) \;=\; & \sum_k (\epsilon_k - \mu) \;+\; \frac{|\psi|^2}{G} \;+\; \sum_k \left[\left(\epsilon_k - \mu - \frac{G}{2}\right)\left(a_k^\dagger a_k + a_{\overline{k}}^\dagger a_{\overline{k}} - 1\right)\right] \\ & - \sum_k \left(\psi^* a_k^\dagger a_{\overline{k}}^\dagger + \psi a_{\overline{k}} a_k\right)\;, \end{aligned} \tag{4.26}$$

where we have used Eqs. (4.4) and (4.5). Since the trace is basis independent, one may choose a convenient basis within which to perform the trace. In order to obtain a diagonal representation of the Hamiltonian, we make a Bogoliubov transformation to the quasiparticle operators

$$\begin{aligned} \alpha_k \;&=\; u_k a_k \;-\; v_k a_{\overline{k}}^\dagger \\ \alpha_{\overline{k}}^\dagger \;&=\; u_k^* a_{\overline{k}}^\dagger \;+\; v_k^* a_k \end{aligned} \tag{4.27}$$

with inverse transformation

$$\begin{aligned} a_k \;&=\; u_k^* \alpha_k \;+\; v_k \alpha_{\overline{k}}^\dagger \\ a_{\overline{k}} \;&=\; u_k^* \alpha_{\overline{k}} \;-\; v_k \alpha_k^\dagger\;, \end{aligned} \tag{4.28}$$

and

$$|u_k|^2 \;+\; |v_k|^2 \;=\; 1\;, \tag{4.29}$$

to conserve fermion anticommutation relations. With the use of the inverse transformation (4.28), we may write

$$a_k^\dagger a_k \;=\; \left(u_k \alpha_k^\dagger \;+\; v_k^* \alpha_{\overline{k}}\right)\left(u_k^* \alpha_k \;+\; v_k \alpha_{\overline{k}}^\dagger\right)$$

$$
\begin{aligned}
&= |u_k|^2\alpha_k^\dagger\alpha_k + u_kv_k\alpha_k^\dagger\alpha_{\bar{k}}^\dagger + u_k^*v_k^*\alpha_{\bar{k}}\alpha_k + |v_k|^2\alpha_{\bar{k}}\alpha_{\bar{k}}^\dagger \\
&= |v_k|^2 + |u_k|^2\alpha_k^\dagger\alpha_k + u_kv_k\alpha_k^\dagger\alpha_{\bar{k}}^\dagger + u_k^*v_k^*\alpha_{\bar{k}}\alpha_k - |v_k|^2\alpha_{\bar{k}}^\dagger\alpha_{\bar{k}} \\
a_{\bar{k}}^\dagger a_{\bar{k}} &= \left(u_k\alpha_{\bar{k}}^\dagger - v_k^*\alpha_k\right)\left(u_k^*\alpha_{\bar{k}} - v_k\alpha_k^\dagger\right) \\
&= |u_k|^2\alpha_{\bar{k}}^\dagger\alpha_{\bar{k}} - u_kv_k\alpha_{\bar{k}}^\dagger\alpha_k^\dagger - u_k^*v_k^*\alpha_k\alpha_{\bar{k}} + |v_k|^2\alpha_k\alpha_k^\dagger \\
&= |v_k|^2 + |u_k|^2\alpha_{\bar{k}}^\dagger\alpha_{\bar{k}} + u_kv_k\alpha_k^\dagger\alpha_{\bar{k}}^\dagger + u_k^*v_k^*\alpha_{\bar{k}}\alpha_k - |v_k|^2\alpha_k^\dagger\alpha_k \\
a_k^\dagger a_{\bar{k}}^\dagger &= \left(u_k\alpha_k^\dagger + v_k^*\alpha_{\bar{k}}\right)\left(u_k\alpha_{\bar{k}}^\dagger - v_k^*\alpha_k\right) \\
&= u_k^2\alpha_k^\dagger\alpha_{\bar{k}}^\dagger - v_k^{*2}\alpha_{\bar{k}}\alpha_k + u_kv_k^* - u_kv_k^*\left(\alpha_k^\dagger\alpha_k + \alpha_{\bar{k}}^\dagger\alpha_{\bar{k}}\right) \\
a_{\bar{k}}a_k &= \left(u_k^*\alpha_{\bar{k}} - v_k\alpha_k^\dagger\right)\left(u_k^*\alpha_k + v_k\alpha_{\bar{k}}^\dagger\right) \\
&= u_k^{*2}\alpha_{\bar{k}}\alpha_k - v_k^2\alpha_k^\dagger\alpha_{\bar{k}}^\dagger + u_k^*v_k - u_k^*v_k\left(\alpha_k^\dagger\alpha_k + \alpha_{\bar{k}}^\dagger\alpha_{\bar{k}}\right) , \qquad (4.30)
\end{aligned}
$$

so that

$$
\begin{aligned}
a_k^\dagger a_k + a_{\bar{k}}^\dagger a_{\bar{k}} &= 2|v_k|^2 + \left(|u_k|^2 - |v_k|^2\right)\left(\alpha_{\bar{k}}^\dagger\alpha_{\bar{k}} + \alpha_k^\dagger\alpha_k\right) \\
&\quad + 2\left(u_kv_k\alpha_k^\dagger\alpha_{\bar{k}}^\dagger + u_k^*v_k^*\alpha_{\bar{k}}\alpha_k\right) \\
\psi^*a_k^\dagger a_{\bar{k}}^\dagger + \psi a_{\bar{k}}a_k &= \left(\psi^*u_k^2 - \psi v_k^2\right)\alpha_k^\dagger\alpha_{\bar{k}}^\dagger + \left(\psi u_k^{*2} - \psi^*v_k^{*2}\right)\alpha_{\bar{k}}\alpha_k \\
&\quad - \left(\psi^*u_kv_k^* + \psi u_k^*v_k\right)\left(\alpha_{\bar{k}}^\dagger\alpha_{\bar{k}} + \alpha_k^\dagger\alpha_k - 1\right) . \qquad (4.31)
\end{aligned}
$$

We now choose the transformation parameters u_k and v_k such that

$$
\begin{aligned}
2\left(\epsilon_k - \mu - \frac{G}{2}\right)u_kv_k - \left(\psi^*u_k^2 - \psi v_k^2\right) &= 0 \\
2\left(\epsilon_k - \mu - \frac{G}{2}\right)u_k^*v_k^* - \left(\psi u_k^{*2} - \psi^*v_k^{*2}\right) &= 0 . \qquad (4.32)
\end{aligned}
$$

With this choice, u_k and v_k may be taken as real variables, and equation (4.26) then becomes

$$
\begin{aligned}
h(\psi) &= \sum_k \left[\left(\epsilon_k - \mu - \frac{G}{2}\right)\left(u_k^2 - v_k^2\right) + 2|\psi|u_kv_k\right]\left(\alpha_k^\dagger\alpha_k + \alpha_{\bar{k}}^\dagger\alpha_{\bar{k}} - 1\right) \\
&\quad + \sum_k \left(\epsilon_k - \mu\right) + \frac{|\psi|^2}{G} . \qquad (4.33)
\end{aligned}
$$

It is readily verified that

$$\begin{aligned} u_k^2 &= \frac{1}{2}\left[1 + \frac{(\epsilon_k - \mu - \frac{G}{2})}{R_k}\right] \\ v_k^2 &= \frac{1}{2}\left[1 - \frac{(\epsilon_k - \mu - \frac{G}{2})}{R_k}\right] \end{aligned} \tag{4.34}$$

with

$$R_k = \sqrt{\left(\epsilon_k - \mu - \frac{G}{2}\right)^2 + |\psi|^2}\,, \tag{4.35}$$

satisfies the requirement (4.32), and upon substituting this form into Eq. (4.33), one obtains

$$h(\psi) = \sum_k (\epsilon_k - \mu) + \frac{|\psi|^2}{G} + \sum_k R_k \left(\alpha_k^\dagger \alpha_k + \alpha_{\bar{k}}^\dagger \alpha_{\bar{k}} - 1\right)\,. \tag{4.36}$$

Since we now have a diagonal representation of the Hamiltonian in quasiparticle space, the required trace is readily evaluated. One may write

$$\begin{aligned} \mathrm{Tr}\left[e^{-\beta h(\psi)}\right] &= e^{\left\{\sum_k (-\beta\epsilon_k + \alpha + \beta R_k) - \beta\frac{|\psi|^2}{G}\right\}} \mathrm{Tr} e^{-\beta\sum_k R_k\left(\alpha_k^\dagger\alpha_k + \alpha_{\bar{k}}^\dagger\alpha_{\bar{k}}\right)} \\ &= e^{\left\{\sum_k (-\beta\epsilon_k + \alpha + \beta R_k) - \beta\frac{|\psi|^2}{G}\right\}} \mathrm{Tr}\prod_k e^{-\beta R_k\left(\alpha_k^\dagger\alpha_k + \alpha_{\bar{k}}^\dagger\alpha_{\bar{k}}\right)} \\ &= e^{\left\{\sum_k (-\beta\epsilon_k + \alpha + \beta R_k) - \beta\frac{|\psi|^2}{G}\right\}} \prod_k \left(1 + e^{-\beta R_k}\right)^2 \\ &= e^{\left\{\sum_k \left[-\beta\epsilon_k + \alpha + \beta R_k + 2\ln\left(1+e^{-\beta R_k}\right)\right] - \beta\frac{|\psi|^2}{G}\right\}}\,, \end{aligned} \tag{4.37}$$

where we have used the fact that the operators $\alpha_k^\dagger\alpha_k$ commute for different k. Finally, we make the substitution $\psi = \Delta e^{i\theta}$, and obtain for the grand partition function in the SPA

$$\mathcal{Z}(\beta,\alpha)_{SPA} = \beta\int_0^\infty d\left(\frac{\Delta^2}{G}\right)\; e^{-\beta\Omega\left(\frac{\Delta^2}{G}\right)}\,, \tag{4.38}$$

with

$$\begin{aligned} \beta\Omega &= \sum_k \left[\beta\epsilon_k - \alpha - S_k - 2\ln\left(1+e^{-S_k}\right)\right] + \frac{\beta\Delta^2}{G} \\ S_k &= \beta R_k = \sqrt{Q_k^2 + \beta^2\Delta^2} \\ Q_k &= \beta\epsilon_k - \alpha - \frac{1}{2}\beta G \ . \end{aligned} \tag{4.39}$$

4.3 Thermodynamic fluctuations in finite systems

In the thermodynamic limit, $N, V \to \infty$ with the density $\frac{N}{V}$ finite, the equilibrium state of a system is given by its most probable configuration, and thermodynamic fluctuations of the system into other states are negligible. In finite systems, however, thermal fluctuations can cause large deviations from the most probable configuration, since these fluctuations are of order $\frac{1}{\sqrt{N}}$. Thus the average and most probable values of an observable do not necessarily coincide, as the equilibrium distribution of the system differs from the most probable state [42]. Mean field theories such as the finite temperature BCS formalism assume the system to be in its most probable state, and are therefore inadequate for the description of small systems such as superconducting grains [25], or the pairing phase transition that takes place in hot nuclei [8].

Besides the functional integral representation, other representations of the partition function exist which also allow for the inclusion of thermodynamic fluctuations in finite systems. Amongst these is the Landau formalism, in which one assumes that the macroscopic state of a system can be characterized by a single macroscopic order parameter ξ. According to the fundamental postulate of statistical mechanics, all accessible states of a system at a given temperature are equally probable. Thus the probability $P(\xi)$ that a particular value of ξ is measured will be proportional to the number of available states with that value of ξ. For a system at given inverse temperature β, this probability is proportional to the partition function for this particular value of ξ, *viz.*

$$P(\xi) \propto \mathcal{Z}(\xi) = e^{-\beta\Omega(\xi)} \ , \tag{4.40}$$

with Ω the thermodynamic potential of the system. In the mean-field formalism, the system is assumed to be in the state which minimizes Ω, that is, the most probable state. Thus the expectation value of an observable, such as the order parameter, is simply given by its value in the state which minimizes Ω. This is valid in the thermodynamic limit, as explained above. For finite systems, however, the expectation value of the order parameter must be determined as a thermal average according to

$$\begin{aligned} \bar{\xi} &= \frac{\int_0^\infty d\xi\ \xi\ P(\xi)}{\int_0^\infty d\xi\ P(\xi)} \\ &= \frac{\int_0^\infty d\xi\ \xi\ e^{-\beta\Omega(\xi)}}{\int_0^\infty d\xi\ e^{-\beta\Omega(\xi)}}\ , \end{aligned} \tag{4.41}$$

which in general differs from the most probable value. The mean square fluctuation in ξ given by

$$\Delta\xi = \sqrt{\overline{\xi^2} - \bar{\xi}^2}\ . \tag{4.42}$$

Clearly the total partition function is then given by

$$\mathcal{Z} = \frac{1}{\gamma}\int_0^\infty d\xi\ \mathcal{Z}(\xi) = \frac{1}{\gamma}\int_0^\infty d\xi\ e^{-\beta\Omega(\xi)}\ , \tag{4.43}$$

with γ a normalization constant. In general, the expectation value of an observable represented by an operator O is then determined according to the relation

$$\begin{aligned} \bar{O} &= \frac{\int_0^\infty d\xi\ \ O(\xi)\mathcal{Z}(\xi)}{\int_0^\infty d\xi\ \mathcal{Z}(\xi)} \\ &= \frac{\int_0^\infty d\xi\ O(\xi)\ e^{-\beta\Omega(\xi)}}{\int_0^\infty d\xi\ e^{-\beta\Omega(\xi)}}\ . \end{aligned} \tag{4.44}$$

Comparing the form (4.43) with the functional integral representation of the grand partition function evaluated in the SPA (4.38), it is clear that the SPA accounts for thermodynamic fluctuations of the system into states other than the most probable state, via a thermal averaging process. If the integrand of equation (4.38) is minimized with respect to Δ, one obtains

$$\Delta = \frac{G}{2}\sum_k \frac{\partial R_k}{\partial\Delta}\left(1 - \frac{2}{1+e^{\beta R_k}}\right) \tag{4.45}$$

so that

$$1 = \frac{G}{2}\sum_k \frac{1-2f_k}{R_k}\,, \tag{4.46}$$

with $f_k = \frac{1}{1+e^{\beta R_k}}$ the occupation probability of the quasiparticle state with energy R_k. This is clearly a reproduction of the finite temperature BCS gap equation (2.54), and thus corresponds to a mean-field treatment where the system is assumed to be in its most probable state.

4.4 The order parameter for pairing systems

Traditionally the order parameter for a system governed by a Hamiltonian of the form (4.3) is chosen to be the gap parameter defined as

$$\Delta \equiv G\sum_k < a_{\bar{k}}a_k > \ . \tag{4.47}$$

Note that this definition is consistent with our previous definition of the finite temperature BCS gap (2.53), since

$$< a_{\bar{k}}a_k > = u_k v_k\,(1-2f_k)\ , \tag{4.48}$$

with f_k as before. For a second order phase transition such as the transition from the pairing to the normal state, the order parameter should approach zero smoothly at the critical temperature. In a mean-field treatment the BCS gap does indeed remain finite below the critical temperature, and approach zero at T_c, both in the thermodynamic limit, and for finite systems. However, if instead the thermal average of the gap is calculated in order to include statistical fluctuations in finite systems, this average is found to remain nonzero above the critical temperature [42, 8]. Thus the second order phase transition is "washed out" by the thermodynamic fluctuations.

The choice of the BCS gap as the order parameter suffers from several drawbacks. Firstly, in an exact canonical calculation, where the number of particles is strictly conserved, it is clear from the definition of the gap that it is uniformly zero on both sides of the phase transition. Furthermore, for a momentum dependent pairing interaction, with the Hamiltonian given by

$$H = \sum_k \epsilon_k \left(a_k^\dagger a_k + a_{\bar{k}}^\dagger a_{\bar{k}}\right) - \sum_{k,k'} G_{k,k'}\, a_k^\dagger a_{\bar{k}}^\dagger a_{\bar{k'}} a_{k'}\ , \tag{4.49}$$

the gap also becomes momentum dependent, and is no longer a single parameter characterizing the macroscopic state of the system. Thus an alternative choice for the order parameter is required.

The comparison of Eqs (4.43) and (4.38) leads one to identify $\mathcal{G} = \frac{\Delta^2}{G}$ as the order parameter for a finite system. For a momentum independent pairing potential (4.52), and in the thermodynamic limit, this is equivalent to choosing the expectation value of the pairing potential for the order parameter, i.e.

$$\mathcal{G} = G \sum_{k,k'} \left\langle a_k^\dagger a_{\bar{k}}^\dagger a_{\bar{k}'} a_{k'} \right\rangle . \tag{4.50}$$

We shall see that in the thermodynamic limit, $\mathcal{G}$ behaves in a similar manner to the BCS gap, approaching zero smoothly at T_c. However, the parameter $\mathcal{G}$ remains macroscopically well defined for momentum dependent pairing potentials, and is also well behaved in an exact treatment. Surprisingly, for finite systems $\mathcal{G}$ remains finite above the transition temperature, even when thermal fluctuations are *not* included.

In order to calculate the partition function with $\mathcal{G}$ as the order parameter, we again perform the Bogoliubov transformation (4.27) to quasiparticle space. The fact that we may choose the transformation parameters u_k and v_k to be real, together with the constraint $u_k^2 + v_k^2 = 1$, allows one to replace these two variables by a single parameter x_k defined by

$$\left.\begin{matrix} u_k^2 \\ v_k^2 \end{matrix}\right\} = \frac{1}{2}(1 \pm x_k) . \tag{4.51}$$

The expectation value of the Hamiltonian

$$H = \sum_k \epsilon_k \left(a_k^\dagger a_k + a_{\bar{k}}^\dagger a_{\bar{k}} \right) - G \sum_{k,k'} a_k^\dagger a_{\bar{k}}^\dagger a_{\bar{k}'} a_{k'} \tag{4.52}$$

is now given by

$$\mathcal{E} = < E > = 2 \sum_k \epsilon_k \rho_k - G \sum_{k,k'} \tau_k^* \tau_{k'} - G \sum_k \rho_k^2 , \tag{4.53}$$

where ρ_k is the single particle density

$$\rho_k = < a_k^\dagger a_k > = < a_{\bar{k}}^\dagger a_{\bar{k}} > = \frac{1}{2}\left[1 - x_k(1 - 2f_k)\right] , \tag{4.54}$$

with

$$f_k \; = < \alpha_k^\dagger \alpha_k > = < \alpha_{\bar{k}}^\dagger \alpha_{\bar{k}} > \, , \tag{4.55}$$

and the quantity

$$\tau_k \; = < a_{\bar{k}} a_k > = \; u_k v_k \; (1 - 2 f_k) \; = \; \frac{1}{2} \sqrt{1 - x_k^2} \; (1 - 2 f_k) \; , \tag{4.56}$$

is defined as the pairing tensor. In the thermodynamic limit, the contribution from the third term in equation (4.53), which we denote by $\mathcal{T}_3$, vanishes. To see this, note that in this limit the density of the single particle levels is sufficiently high that we may replace the sum over momenta by an integral, according to

$$\sum_k \; \rightarrow \; \frac{V}{(2\pi)^3} \int d^3 k \; . \tag{4.57}$$

Note further that $G = \frac{g}{V}$ is the strength of the pairing interaction per unit volume, with g the dimensionless interaction strength. Thus, in calculating the energy per unit volume $\frac{\mathcal{E}}{V}$, which is a finite quantity in the thermodynamic limit, the term $\frac{\mathcal{T}_3}{V}$ is of order $\frac{1}{V}$, or equivalently of order $\frac{1}{N}$. Therefore in the limit $N, V \; \rightarrow \; \infty$ with the density $\frac{N}{V}$ constant, the contribution from $\mathcal{T}_3$ vanishes. Thus in the thermodynamic limit one may ignore this term, and we find

$$\mathcal{G} \; = \; G \sum_{k,k'} \tau_k^* \tau_{k'} \; = \; \frac{\Delta^2}{G} \; , \tag{4.58}$$

so that $\mathcal{G}$ tends to zero as the critical temperature is approached. In finite systems, however, the contribution from $\mathcal{T}_3$ remains nonzero, and $\mathcal{G}$ remains finite above the phase transition, even before the effect of thermal fluctuations has been included.

To calculate the partition function as a function of the order parameter $\mathcal{G}$ we minimize the free energy $F = \mathcal{E} - TS$ with respect to the transformation parameters x_k and the quasiparticle occupation probabilities f_k, subject to the constraints that

$$\mathcal{G} \; = \; G \left[\sum_{k,k'} \tau_k^* \tau_{k'} \; + \; G \sum_k \rho_k^2 \right] \; , \tag{4.59}$$

and that the number of particles is given by

$$\mathcal{N} \; = < N > = \; 2 \sum_k \rho_k \; , \tag{4.60}$$

which fixes the average number of particles. In order the incorporate these constraints, we define

$$\begin{aligned} F' &= F - \mu\mathcal{N} - \lambda\mathcal{G} \\ &= \mathcal{E} - T < S > - \mu\mathcal{N} - \lambda\mathcal{G} \, . \end{aligned} \tag{4.61}$$

Here λ and the chemical potential μ act as Lagrange multipliers. The entropy $< S >$ is given by the Fermi-Dirac expression

$$< S > = -2k_B \sum_k \left[f_k \ln f_k + (1 - f_k) \ln (1 - f_k) \right] \, . \tag{4.62}$$

The minimization of F' with respect to x_k yields

$$x_k = \frac{\epsilon'_k}{\sqrt{\epsilon'^2_k + \Delta'^2}} \tag{4.63}$$

with

$$\epsilon'_k = \epsilon_k - \frac{G}{2} (1 + \lambda) \, \rho_k \tag{4.64}$$

and

$$\Delta' = G \, (1 + \lambda) \sum_k \tau_k \, . \tag{4.65}$$

Minimizing F' with respect to f_k one obtains the corrected form for the quasiparticle occupation probabilities

$$f_k = \frac{1}{1 + \exp\left(\beta \sqrt{\epsilon'^2_k + \Delta'^2}\right)} \, . \tag{4.66}$$

Equations (4.59), (4.60) and (4.63)-(4.66) are now solved simultaneously for Δ', μ and λ to obtain F' as a function of $\mathcal{G}$, whereupon the partition function in the order parameter representation is given by

$$\mathcal{Z}_{ord} = \frac{1}{\gamma} \int_0^\infty d\mathcal{G} \; e^{-\beta\Omega(\mathcal{G})} \, , \tag{4.67}$$

with $\Omega = F - \mu N$ the thermodynamic potential. The normalization constant γ cancels in the calculation of the thermodynamic properties of the

system, as is apparent from Eq. (4.44). The energy of the system now follows from the partition function in straightforward manner, according to

$$E = -\frac{\partial \ln \mathcal{Z}}{\partial \beta} . \tag{4.68}$$

The heat capacity with fixed average number of particles, C_N, can be obtained either as the numerical derivative of a fit to the energy

$$C_N = \left(\frac{\partial E}{\partial T}\right)_{\overline{N},V} , \tag{4.69}$$

or analytically according to the relation [43]

$$C_N = \frac{\overline{(\Delta E)^2}}{k_B T^2} - \frac{\overline{(\Delta N)^2}}{k_B T^2}\left(\frac{\partial \alpha}{\partial \beta}\right)_N^2 , \tag{4.70}$$

with

$$\left(\frac{\partial \alpha}{\partial \beta}\right)_N = \frac{-\left(EN + \frac{1}{\mathcal{Z}}\frac{\partial^2 \mathcal{Z}}{\partial \beta \partial \alpha}\right)}{\overline{(\Delta N)^2}} , \tag{4.71}$$

and the energy and number fluctuations, $\overline{(\Delta E)^2}$ and $\overline{(\Delta N)^2}$ respectively, given by

$$\begin{aligned} \overline{(\Delta E)^2} &= \overline{E^2} - \overline{E}^2 = \frac{\partial^2 \ln \mathcal{Z}}{\partial^2 \beta} , \\ \overline{(\Delta N)^2} &= \overline{N^2} - \overline{N}^2 = \frac{\partial^2 \ln \mathcal{Z}}{\partial^2 \alpha} . \end{aligned} \tag{4.72}$$

As a check, we have applied both methods of calculating the heat capacity in the grand canonical ensemble, with identical results.

Fig 4.1 shows the expectation value of the potential as a function of temperature. These calculations were performed in the $i_{\frac{13}{2}}$ model, a simple nuclear model discussed in Appendix A, which permits the calculation of exact grand canonical results. In the conventional mean-field BCS approach in the thermodynamic limit, the third term in equation (4.53) is ignored, and $\mathcal{G}$ tends to zero at the transition temperature T_c, as it should. However, if the third term in Eq. (4.53) is included, $\mathcal{G}$ remains finite above T_c, even without

the effect of thermal fluctuations. Applying the Landau formalism in order to include thermodynamic fluctuations, it is clear that the phase transition is smoothed out by the fluctuations, due to the finite size of the system. Note also that using $\mathcal{G}$ for the order parameter in the Landau approach, rather than the BCS gap, gives better quantitative agreement with the exact grand canonical result. The remaining errors are mainly due to the neglect of non-thermodynamic fluctuations.

In Fig 4.2 the heat capacity is plotted as a function of temperature. As expected, the standard mean-field BCS result shows a discontinuity at the second order phase transition. The SPA and the Landau treatment both include the effect of thermodynamic fluctuations, which smooths out the discontinuity in the specific heat. The SPA and the Landau approach with $\mathcal{G}$ as the order parameter give very similar results. Both these methods predict a critical temperature very close to the exact grand canonical result, although they underestimate the height of the peak in the heat capacity. Using the BCS gap for the order parameter, one finds that the height of the peak in the specific heat compares well with the exact result, but that the prediction of the peak position is rather poor. Acknowledgement is due to Fritz Solms for all the results in Figs. 4.1 and 4.2, with the exception of the results obtained using the Landau approach with $\mathcal{G}$ as the order parameter, which are due to the author.

Thus the choice of $\mathcal{G}$ as the Landau order parameter for a finite system instead of the more conventional BCS energy gap not only resolves the conceptual difficulties encountered with the latter choice, but also yields a better approximation to the expectation value of the pairing potential. Furthermore, one obtains a more accurate prediction of the position of the peak in the heat capacity. The peak position is usually more important than the peak height, since the position of the peak in the heat capacity indicates the critical temperature for the pairing phase transition. Using the expectation value of the potential as the order parameter, one obtains results very similar to the results in the static path approximation, which further indicates that the SPA corresponds to the inclusion of thermodynamic fluctuations. For a finite system governed by a BCS-like pairing Hamiltonian, the expectation value of the potential seems to be a good choice for the order parameter of the system in the Landau treatment. For other potentials, which might include non-pairing terms in the Hamiltonian, a simple generalization of this choice is not clear.

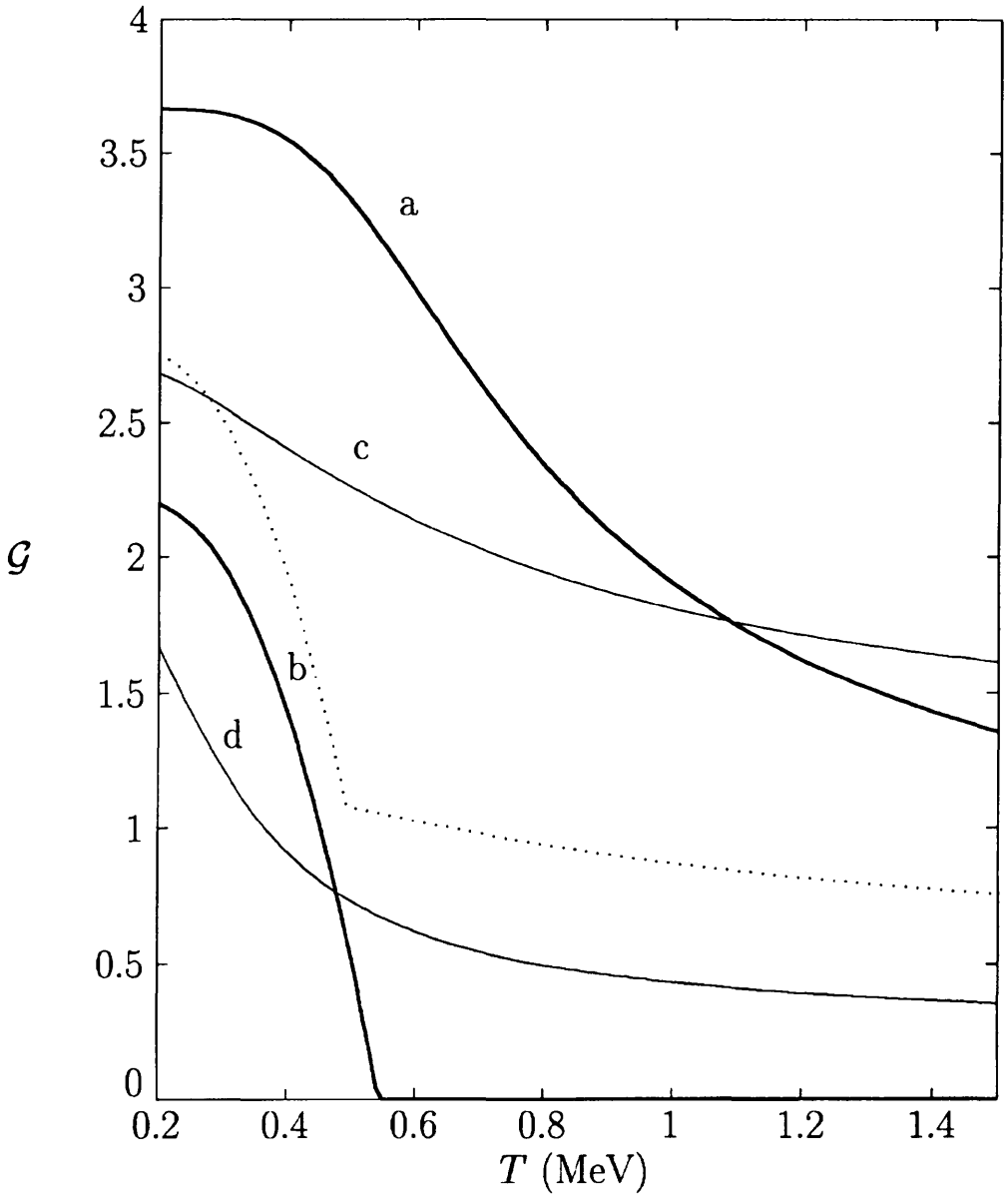

Figure 4.1: The expectation value of the potential, $\mathcal{G}$, in the exact grand canonical ensemble (thick solid line labelled a), in the conventional mean-field BCS approach (thick solid line labelled b), in the mean-field BCS approach including the third term in equation (4.53) (dotted line), and in the Landau formalism using $\mathcal{G}$ (thin solid line marked c) and the BCS energy gap (thin solid line marked d) for the order parameter.

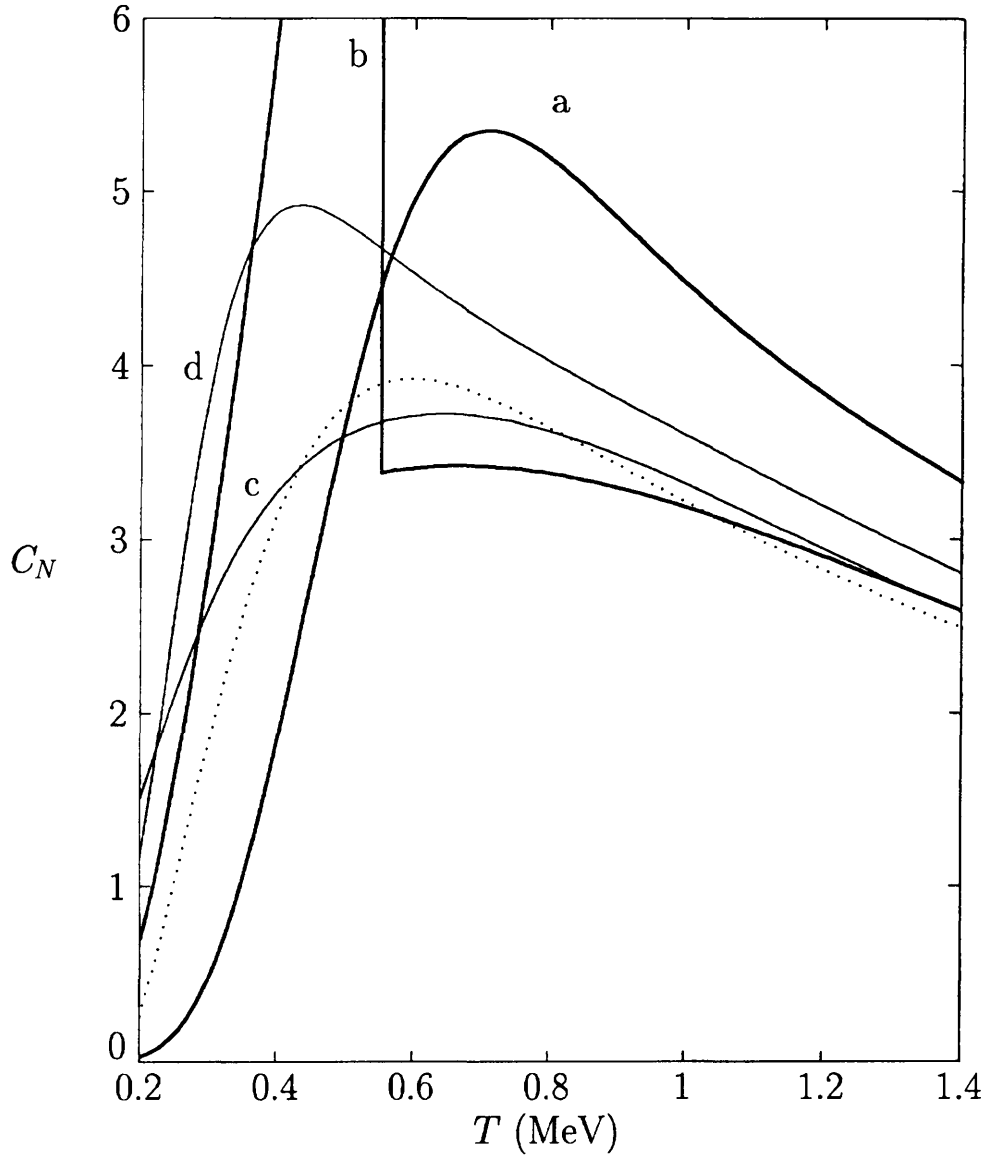

Figure 4.2: The heat capacity with fixed average number of particles, C_N, as a function of temperature. The thick solid line labelled a gives the exact grand canonical result, the thick solid line labelled b is the standard BCS mean-field result, the dotted line gives the result from the SPA approach, the thin solid line labelled c shows the result obtained from the Landau theory using $\mathcal{G}$ for the order parameter, and the thin solid line labelled d gives the result using the BCS gap for the order parameter. Note that we have chosen units such that $k_B = 1$ throughout, so that the heat capacity is dimensionless.

4.5 The RPA-SPA approximation to the grand partition function

It is clear from the form of the partition function in the SPA that this approximation includes thermodynamic fluctuations. In the BCS formalism, however, non-thermodynamic fluctuations also arise. These *quantum* fluctuations occur firstly due to the fact that the BCS ground state is not the exact ground state of the system. In particular, the BCS state violates the particle number symmetry of the Hamiltonian, thereby inducing fluctuations in the particle number. Furthermore, fluctuations of the system into states other than those compatible with BCS quasiparticle excitation are not considered in a BCS treatment.

The RPA-SPA approximation to the grand partition function, first developed by Puddu *et al.* [39, 40], attempts to remedy this situation. In the RPA-SPA, the fields $\phi_x(t_n)$ and $\phi_y(t_n)$ introduced in equation (4.13) are approximated not only by their zeroth order Fourier components as in the SPA. Rather one also includes the lowest order contributions from all higher order components. These contributions then correspond to small amplitude quantum corrections, or fluctuations, about the static path approximation. A calculation analogous to the SPA goes through, and one obtains for the grand partition function in the RPA-SPA approximation scheme [40]

$$\mathcal{Z}(\beta,\alpha)_{RPA-SPA} = \frac{2\beta}{G}\int_0^\infty d\Delta\ \Delta\ e^{-\beta\Omega(\Delta)}\,\mathcal{C}\ , \tag{4.73}$$

with $\beta\Omega$ as before, and the factor $\mathcal{C}$ given by

$$\mathcal{C} = \prod_{m>0} B_m^{-1} \tag{4.74}$$

with

$$\begin{aligned} B_m = & \left(1-\frac{\beta G}{2}\sum_k \frac{Q_k^2}{S_k}\frac{\tanh\left(\frac{S_k}{2}\right)}{S_k^2+(\pi m)^2}\right)\left(1-\frac{\beta G}{2}\sum_k S_k\frac{\tanh\left(\frac{S_k}{2}\right)}{S_k^2+(\pi m)^2}\right) \\ & + \left(\frac{\beta G}{2}\sum_k \frac{Q_k}{S_k}\frac{(\pi m)\tanh\left(\frac{S_k}{2}\right)}{S_k^2+(\pi m)^2}\right)^2 . \end{aligned} \tag{4.75}$$

with S_k and Q_k as in equations (4.39). Thus, in the RPA-SPA, not only are thermodynamic fluctuations included, but small-amplitude quantal fluctuations are also taken into account via the factor $\mathcal{C}$ defined above. It has been shown [40] that at very low temperatures, large-amplitude quantum corrections also become important. However, at temperatures high enough for these large-amplitude corrections to be negligible, the RPA-SPA approximation (4.73) represents a very good approximation to the exact grand partition function. This can be clearly seen in Fig. 4.3 where the heat capacity has been calculated in the grand canonical ensemble, both exactly and using the RPA-SPA approximation, for average number of particles $N = 6$ and $N = 8$. In both cases, the average error due to the approximation is less than 2 %. This calculation was also performed in the $i_{\frac{13}{2}}$ model. Note again that Eq. (4.73) is in general not valid at very low temperatures, as large amplitude quantal fluctuations may have to be taken into account in this region.

Strictly speaking, these grand canonical calculations are not applicable for a system such as a nucleus, as the number of nucleons is very definitely non-varying. The particle number fluctuations in the grand canonical ensemble provide an indication of whether a canonical calculation, where the particle number is fixed, is required. In our model calculation, these number fluctuations (4.72) are appreciable (see Table 5.1). Therefore, in chapter 5, we consider means of obtaining the more appropriate canonical results for small pairing systems.

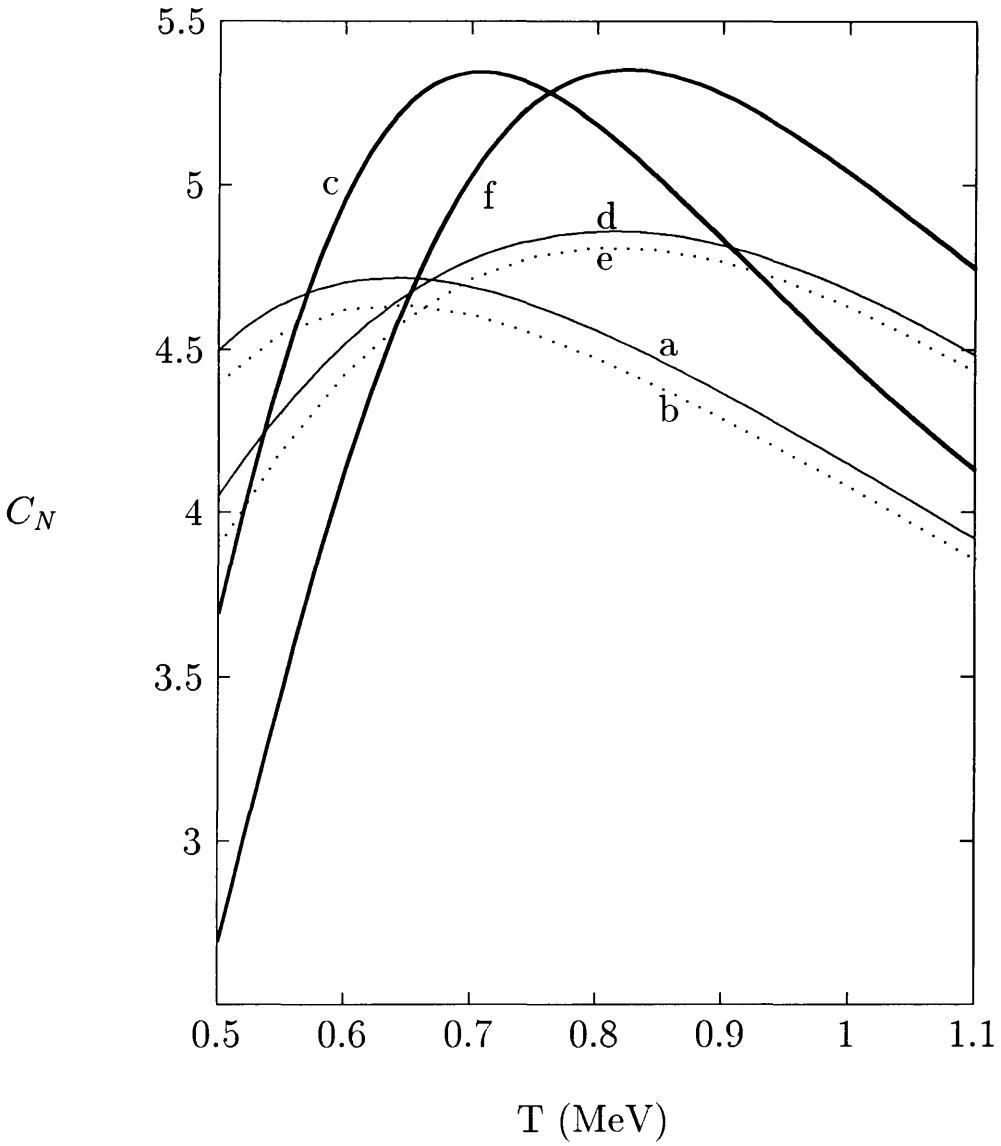

Figure 4.3: The heat capacity as a function of temperature, calculated from the exact grand canonical partition function (thin solid lines), from the RPA-SPA path integral approximation to the grand partition function (dotted lines), and in the exact canonical ensemble (thick solid lines). The results for $N = 6$ are labelled a, b and c, and the results for $N = 8$ are labelled d, e and f, respectively.

Chapter 5

Canonical Number Projection

5.1 An introduction to number projection

For a finite system the number of particles in the system is fixed and any calculation of the properties of the system should be performed in the canonical ensemble. Since it is often simpler to do these calculations grand canonically, well-known techniques exist to project the canonical from the grand canonical results [26]. This is particularly useful in a BCS-type calculation, since in the BCS formalism the ground state particle number is variable.

Since exact calculations are often impossible we consider here the results of number projection on a grand partition function which is only approximately determined [27]. To check the results the heat capacity has been calculated in a schematic $i_{\frac{13}{2}}$ pairing model [8], where it is also possible to perform the exact canonical and grand canonical calculations (see Appendix A). The grand partition function has been approximated using a functional integral approach including both thermodynamic and small-amplitude quantal corrections, as discussed in chapter 4. The number projection has been accomplished by inverting the formal expansion of the grand partition function in terms of the canonical partition functions. This inversion has been achieved using both a contour integral and a Chebyschev series inversion, and in both cases is formally exact. However, despite excellent agreement between the approximate and exact grand canonical results, the results of number projection on the approximate grand partition function are disturbingly poor [27].

Both number projection methods described above are independent of the form for the approximation to the grand partition function. It is also possible to develop number projection methods that take into account the manner in which the grand partition function is approximated. This has been done in the context of the static path approximation [44, 45, 46], which only includes thermodynamic, and not quantum fluctuations. In these calculations [44, 45, 46], number projection was found to have little effect, but only the energy and level density were considered. However, we found the energy to be less sensitive to the choice of ensemble than the heat capacity.

Thus, even though number projection is relevant for small systems [47], our results indicate that canonical projection directly from the approximate grand partition function does not yield the pertinent information. The next section describes the number projection techniques, and section 5.3 gives the results and conclusions.

5.2 Canonical number projection techniques

The method of "Wick rotation" entails expanding the grand canonical partition function $\mathcal{Z}$ in terms of the canonical partition functions Z_N

$$\mathcal{Z}(\beta,\alpha) \;=\; \sum_N e^{\alpha N} Z_N(\beta)\,, \tag{5.1}$$

where β denotes the inverse of the temperature i.e. $\beta = (k_B T)^{-1}$, and then replacing $\alpha \equiv \beta\mu$ by $i\phi$ so that

$$\mathcal{Z}(\beta,i\phi) \;=\; \sum_N e^{i\phi N} Z_N(\beta)\,. \tag{5.2}$$

This is simply a Fourier series and therefore the exact canonical partition function for a system of N particles can be projected from the grand canonical in the following manner:

$$Z_N(\beta) \;=\; \frac{1}{2\pi}\int_{-\pi}^{\pi} d\phi\; e^{-iN\phi}\; \mathcal{Z}(\beta,i\phi)\,. \tag{5.3}$$

The symmetric interval in ϕ ensures that the partition function remains real even when using an approximate form for the grand partition function. One

should note that this form is equivalent to the more formal contour integral expression [26]

$$Z_N(\beta) = \frac{1}{2\pi i}\oint dz \frac{\mathcal{Z}(\beta,z)}{z^{N+1}} \tag{5.4}$$

if the contour is chosen to be the unit circle.

Since it may be argued that the approximation to the grand partition function only approximates its behaviour for real α and not throughout the complex plane, an expansion on the real axis has also been considered. The expansion (5.1) forms a power series in $z = e^{\alpha}$

$$\mathcal{Z}(\beta,z) = \sum_N Z_N(\beta) z^N \,, \tag{5.5}$$

which can be rewritten in terms of shifted Chebyschev polynomials of the first kind T_N^* [48]

$$\mathcal{Z}(\beta,\overline{z}) = \sum_N c_N(\beta)\, T_N^*(\overline{z}) \,, \tag{5.6}$$

where $\overline{z} = \frac{z}{z_{max}} \in [0,1]$, and the cutoff z_{max} has been introduced to enable one to do numerical calculations. Since the $T_N^*(\overline{z})$, when weighted by the functions

$$w(\overline{z}) = \frac{1}{\sqrt{\overline{z}-\overline{z}^2}} \tag{5.7}$$

are orthogonal on the interval $[0,1]$, the expansion coefficients c_N are given by

$$\begin{aligned} c_N(\beta) &= \frac{1}{\pi}\int_0^1 d\overline{z}\; T_N^*(\overline{z})\; \mathcal{Z}(\beta,\overline{z})\; w(\overline{z}) \qquad \text{for} \qquad N = 0 \\ &= \frac{2}{\pi}\int_0^1 d\overline{z}\; T_N^*(\overline{z})\; \mathcal{Z}(\beta,\overline{z})\; w(\overline{z}) \qquad \text{for} \qquad N \neq 0 \,. \end{aligned} \tag{5.8}$$

Comparing Eqs. (5.5) and (5.6), it follows immediately that the coefficients $\{c_N\}$ yield the canonical partition function for N particles through a simple transformation. We remark here that the Chebyschev method, although valid for a system with any number of particles, becomes numerically intractable for large systems due to the magnitude of the terms which contribute to the grand partition function in Eq. (5.5).

The energy E_N can now be calculated from the standard thermodynamic relation

$$E_N = -\frac{1}{Z_N}\left(\frac{\partial Z_N}{\partial \beta}\right)_N . \tag{5.9}$$

In the case of the "Wick rotation" method, $\left(\frac{\partial Z_N(\beta)}{\partial \beta}\right)_N$ is given by

$$\left(\frac{\partial Z_N(\beta)}{\partial \beta}\right)_N = \frac{1}{2\pi}\int_{-\pi}^{\pi} d\phi\, e^{-iN\phi}\,\frac{\partial \mathcal{Z}(\beta, i\phi)}{\partial \beta} , \tag{5.10}$$

where Eq. (5.3) has been used. Using the RPA-SPA approximation to the grand partition function (see Eq. (4.73))

$$\mathcal{Z} = \frac{2\beta}{G}\int_0^{\infty} d\Delta\, \Delta\, e^{-\beta\Omega}\, \mathcal{C} , \tag{5.11}$$

with

$$\begin{aligned} \beta\Omega &= \sum_k \left[\beta\epsilon_k - i\phi - S_k - 2\ln\left(1 + e^{-S_k}\right)\right] + \frac{\beta\Delta^2}{G} \\ S_k &= \sqrt{Q_k^2 + \beta^2\Delta^2} \\ Q_k &= \beta\epsilon_k - i\phi - \frac{1}{2}\beta G \\ \mathcal{C} &= \prod_{m>0} B_m^{-1} \end{aligned} \tag{5.12}$$

and

$$\begin{aligned} B_m = &\left(1 - \frac{\beta G}{2}\sum_k \frac{Q_k^2}{S_k}\frac{\tanh\left(\frac{S_k}{2}\right)}{S_k^2 + (\pi m)^2}\right)\left(1 - \frac{\beta G}{2}\sum_k S_k \frac{\tanh\left(\frac{S_k}{2}\right)}{S_k^2 + (\pi m)^2}\right) \\ &+ \left(\frac{\beta G}{2}\sum_k \frac{Q_k}{S_k}\frac{(\pi m)\tanh\left(\frac{S_k}{2}\right)}{S_k^2 + (\pi m)^2}\right)^2 , \end{aligned} \tag{5.13}$$

the derivative $\frac{\partial \mathcal{Z}(\beta, i\phi)}{\partial \beta}$ is obtained analytically according to

$$\frac{\partial \mathcal{Z}(\beta, i\phi)}{\partial \beta} = \frac{\mathcal{Z}}{\beta} + \frac{2\beta}{G}\int_0^{\infty} d\Delta\, \Delta\, e^{-\beta\Omega}\left(\frac{\partial \mathcal{C}}{\partial \beta} - \mathcal{C}\frac{\partial(\beta\Omega)}{\partial \beta}\right) . \tag{5.14}$$

In the Chebyschev method, one obtains $\left(\frac{\partial Z_N(\beta)}{\partial\beta}\right)_N$ from the expansion

$$\left(\frac{\partial Z_N(\beta)}{\partial\beta}\right)_N = \sum_N \frac{\partial c_N(\beta)}{\partial\beta}\, T_N^*(\overline{z})\,, \tag{5.15}$$

in a similar manner to that used for the partition function. Here the derivatives

$$\begin{aligned}\frac{\partial c_N(\beta)}{\partial\beta} &= \frac{1}{\pi}\int_0^1 d\overline{z}\; T_N^*(\overline{z})\,\frac{\partial\mathcal{Z}(\beta,\overline{z})}{\partial\beta}\,w(\overline{z}) \qquad \text{for} \qquad N=0 \\ &= \frac{2}{\pi}\int_0^1 d\overline{z}\; T_N^*(\overline{z})\,\frac{\partial\mathcal{Z}(\beta,\overline{z})}{\partial\beta}\,w(\overline{z}) \qquad \text{for} \qquad N\neq 0\,,\end{aligned} \tag{5.16}$$

are calculated analytically. In the RPA-SPA approximation, the derivatives $\frac{\partial\mathcal{Z}(\beta,\overline{z})}{\partial\beta}$ are obtained in a similar manner to that for the "Wick" method (see Eq. (5.14)).

In like fashion, one can calculate

$$\overline{E_N^2} = \frac{1}{Z_N}\left(\frac{\partial^2 Z_N}{\partial^2\beta}\right)_N \tag{5.17}$$

analytically. For the Wick rotation, $\left(\frac{\partial^2 Z_N}{\partial^2\beta}\right)_N$ is given by

$$\left(\frac{\partial^2 Z_N(\beta)}{\partial^2\beta}\right)_N = \frac{1}{2\pi}\int_{-\pi}^{\pi} d\phi\; e^{-iN\phi}\,\frac{\partial^2\mathcal{Z}(\beta,i\phi)}{\partial^2\beta}\,. \tag{5.18}$$

In the RPA-SPA approximation (5.11), $\frac{\partial^2\mathcal{Z}(\beta,i\phi)}{\partial^2\beta}$ is obtained analytically according to

$$\begin{aligned}\frac{\partial^2\mathcal{Z}(\beta,i\phi)}{\partial^2\beta} &= \frac{1}{\beta}\frac{\partial\mathcal{Z}(\beta,i\phi)}{\partial\beta} - \frac{\mathcal{Z}}{\beta^2} + \frac{2}{G}\int_0^\infty d\Delta\;\Delta\; e^{-\beta\Omega}\left(\frac{\partial\mathcal{C}}{\partial\beta} - \mathcal{C}\frac{\partial(\beta\Omega)}{\partial\beta}\right) + \\ &\quad \frac{2\beta}{G}\int_0^\infty d\Delta\;\Delta\; e^{-\beta\Omega}\left(\frac{\partial^2\mathcal{C}}{\partial^2\beta} - 2\frac{\partial\mathcal{C}}{\partial\beta}\frac{\partial(\beta\Omega)}{\partial\beta} + \mathcal{C}\left[\frac{\partial(\beta\Omega)}{\partial\beta}\right]^2 - \mathcal{C}\frac{\partial^2(\beta\Omega)}{\partial^2\beta}\right) \\ &= \frac{2}{\beta}\frac{\partial\mathcal{Z}(\beta,i\phi)}{\partial\beta} - \frac{2\mathcal{Z}}{\beta^2} + \frac{2\beta}{G}\int_0^\infty d\Delta\;\Delta\; e^{-\beta\Omega}\times \\ &\quad \left(\frac{\partial^2\mathcal{C}}{\partial^2\beta} - 2\frac{\partial\mathcal{C}}{\partial\beta}\frac{\partial(\beta\Omega)}{\partial\beta} + \mathcal{C}\left[\frac{\partial(\beta\Omega)}{\partial\beta}\right]^2 - \mathcal{C}\frac{\partial^2(\beta\Omega)}{\partial^2\beta}\right)\,,\end{aligned} \tag{5.19}$$

where we have used Eq. (5.14). For the Chebyschev method, one obtains $\left(\frac{\partial^2 Z_N(\beta)}{\partial^2 \beta}\right)_N$ from the expansion

$$\left(\frac{\partial^2 Z_N(\beta)}{\partial^2 \beta}\right)_N = \sum_N \frac{\partial^2 c_N(\beta)}{\partial^2 \beta} T_N^*(\overline{z}) \,, \tag{5.20}$$

again in a similar manner to that used for the partition function. Here the derivatives

$$\begin{aligned} \frac{\partial^2 c_N(\beta)}{\partial^2 \beta} &= \frac{1}{\pi} \int_0^1 d\overline{z}\; T_N^*(\overline{z})\, \frac{\partial^2 \mathcal{Z}(\beta,\overline{z})}{\partial^2 \beta}\, w(\overline{z}) \quad \text{for} \quad N = 0 \\ &= \frac{2}{\pi} \int_0^1 d\overline{z}\; T_N^*(\overline{z})\, \frac{\partial^2 \mathcal{Z}(\beta,\overline{z})}{\partial^2 \beta}\, w(\overline{z}) \quad \text{for} \quad N \neq 0 \,. \end{aligned} \tag{5.21}$$

are calculated analytically. In the RPA-SPA approximation, the derivatives $\frac{\partial^2 \mathcal{Z}(\beta,\overline{z})}{\partial^2 \beta}$ are again obtained in a similar manner to that used for the "Wick rotation" (see Eq. (5.19)).

The heat capacity for a system with fixed particle number is then given by

$$\begin{aligned} C_N &= \frac{\overline{(\Delta E_N)^2}}{k_B T^2} \\ &= \frac{\overline{E_N^2} - \overline{E_N}^2}{k_B T^2} \,. \end{aligned} \tag{5.22}$$

5.3 Results and Conclusions

Calculating the heat capacity C_N for $N = 6$ nucleons in the exact canonical, as opposed to the exact grand canonical ensemble, one finds that the peak in C_N exhibits approximately an 11 % shift towards a higher temperature, and a 13 % increase in height. For eight nucleons there is virtually no shift in the position of the peak, whilst the height increases by only about 10 % (see Fig 4.3). This decrease is to be expected, since the change in the properties of a system in going from a grand canonical to a canonical calculation should be less pronounced for a system with more particles. The relative mean- square fluctuations in the particle number are given in Table 5.1. The fluctuations

Table 5.1: The relative mean-square fluctuation $\frac{\Delta N}{N}$ in the particle number in the grand canonical ensemble, expresses as a percentage, for $N = 6$ and $N = 8$ particles as a function of the temperature, T.

T	$\frac{\Delta N}{N}$ (%)	
	N = 6	N = 8
0.4	16.9	11.2
0.5	18.8	12.6
0.6	20.4	13.9
0.7	21.8	15.0
0.8	23.0	15.9
0.9	23.9	16.8
1.0	24.8	17.5
1.1	25.5	18.2

increase smoothly as a function of the temperature T from 17 % to 26 % for six, and from 11 % to 19 % for eight nucleons, in the temperature range $T = 0.5$ MeV to $T = 1.1$ MeV. Considering the size of these fluctuations it is surprising they do not have a larger effect on the heat capacity of the system.

We applied the number projection methods in the $i_{\frac{13}{2}}$ model, both for $N = 6$ and $N = 8$ nucleons. Substituting the RPA-SPA approximation (5.11) for the grand partition function into Eq. (5.3), we performed the "Wick rotation" to obtain the canonical partition functions, and calculated the energy according to (5.9). The heat capacity as a function of temperature was obtained using equation (5.22). The results for eight and six particles are given in Figs. 5.1 and 5.2, respectively. The results compare poorly with the exact canonical heat capacity, and one finds an average error of 22 % for six, and 11 % for eight particles. Note that the results of the number projection are not given for temperatures below about 0.5 MeV, since, as has been mentioned before, the approximation (5.11) for the grand partition function is not valid in this region.

We have also estimated the numerical errors inherent in the integration for the "Wick rotation", by performing the projection on the exact grand partition function, and comparing the results with the exact canonical heat capacity. The error due to the projection was found to be uniformly less

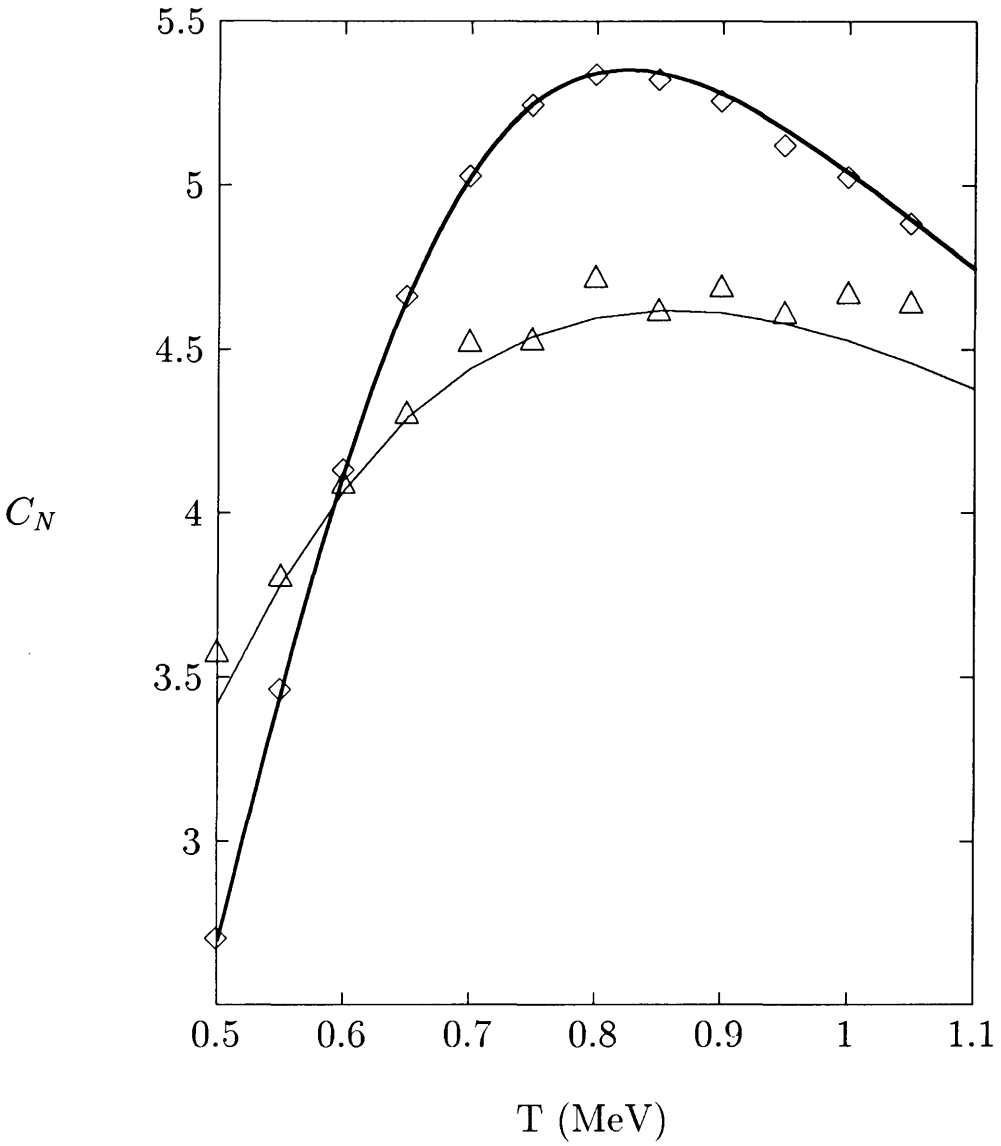

Figure 5.1: The projected heat capacity for $N = 8$ nucleons as a function of temperature, using the "Wick rotation" method applied to the approximate grand partition function (thin solid line), using the Chebyschev expansion method applied to the approximate grand partition function ($\triangle$), and to the exact grand partition function ($\diamond$), and the exact heat capacity calculated in the canonical ensemble (thick solid line).

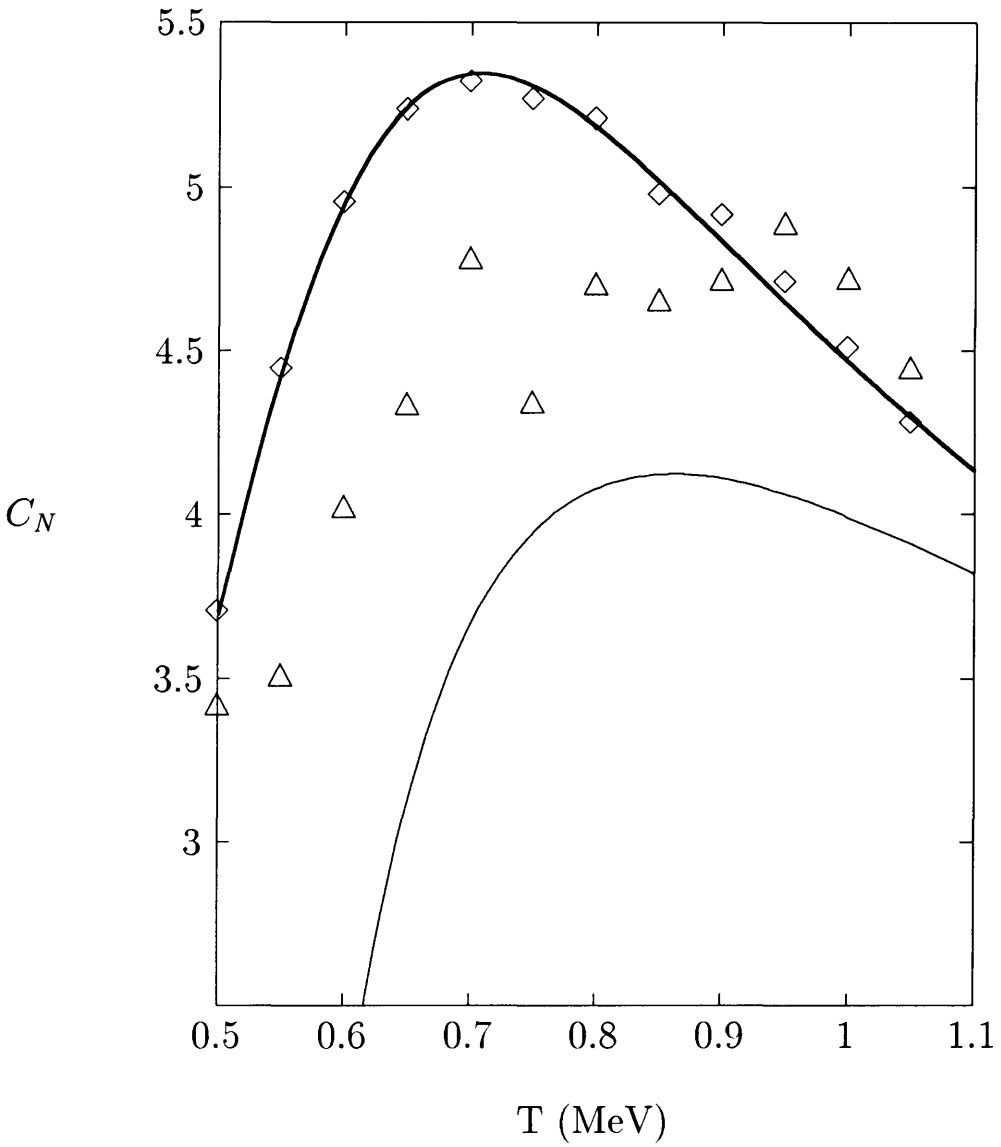

Figure 5.2: The projected heat capacity for $N = 6$ nucleons as a function of temperature, using the "Wick rotation" method applied to the approximate grand partition function (thin solid line), using the Chebyschev expansion method applied to the approximate grand partition function ($\triangle$), and to the exact grand partition function ($\diamond$), and the exact heat capacity calculated in the canonical ensemble (thick solid line).

than 10^{-3} % for both $N = 6$ and $N = 8$ particles over the whole temperature range considered. Thus, for the Wick method, the numerical error due to the projection is entirely negligible, and certainly cannot account for the discrepancy between the exact and approximate projected results.

A similar procedure was followed for the Chebyschev method, but here the choice of the cutoff z_{max} has to be considered. Although it can be formally shown that the results are independent of z_{max} if one uses the exact grand partition function, both numerical errors and the approximation to the partition function introduce some dependence on the cutoff. The numerical errors are mainly due to the magnitude of the quantities involved, in particular the canonical and grand canonical partition functions. For instance, when taking the difference between large numbers, cancellation errors make it difficult to obtain accurate numerical results.

Fortunately, for $N = 8$ particles, there exists a broad easily identifiable region of z_{max} where the heat capacity calculated according to this method is stable with respect to a variation in the cutoff, whilst it fluctuates sharply outside of this interval. This behaviour is illustrated in Table 5.2, where the heat capacity projected from both the exact and the approximate grand partition function via the Chebyschev method is shown as a function of z_{max}, at temperatures $T = 0.65$ MeV and $T = 0.95$ MeV. In our calculation, taking $z_{max} = 4T$ ensures that one obtains stable results for eight particles in the temperature range under consideration. The results for the heat capacity are then given in Fig 5.1. Once again, we have checked the numerical error inherent in the projection method itself by applying the method to the exact grand partition function. The results obtained for $N = 8$ particles in this manner agree uniformly with the exact canonical heat capacity to within 1 % (see Fig. 5.1), and it is clear again that numerical error cannot account for the average error of 10 % in the projected results.

Very similar results are obtained using the Chebyschev method for $N = 6$ particles at low temperatures where again one can identify a broad region of z_{max} for which the projected results are stable (see Table 5.2). Again there is poor agreement with the exact canonical results. However we encountered some numerical instability in the choice of z_{max} at higher temperatures. For the purposes of the calculation of the heat capacity at these temperatures we have simply selected the values of z_{max} to give good results for the projection from the exact grand canonical partition function. Our results are thus less reliable in this case. The results of the Chebyschev projection on

Table 5.2: The heat capacity C_N, projected from the approximate and exact grand partition functions via the Chebyschev method for $N = 6$ and $N = 8$ nucleons, as a function of the cutoff z_{max}, at temperatures $T = 0.95$ and $T = 0.65$.

T	z_{max}	C_N (N=6)		C_N (N=8)	
		Exact	Approximate	Exact	Approximate
0.65	2.0 T	4.42	3.93	3.77	3.70
	3.0 T	5.15	4.42	4.62	4.34
	3.5 T	5.21	4.37	4.65	4.32
	4.0 T	5.23	4.33	4.66	4.30
	4.5 T	5.24	4.42	4.66	4.29
	5.0 T	5.25	4.75	4.67	4.31
	6.0 T	5.26	6.38	4.67	4.45
	10.0 T	7.63	14.0	4.76	5.59
0.95	2.0 T	-0.24	-0.94	0.03	-0.64
	3.0 T	4.18	3.11	4.96	4.15
	3.5 T	4.41	4.47	5.10	4.74
	4.0 T	4.33	3.93	5.12	4.60
	4.5 T	4.68	4.63	5.17	4.78
	5.0 T	4.75	5.01	5.19	4.94
	6.0 T	4.94	7.94	5.23	5.63
	10.0 T	6.16	-7.08	5.76	9.82

the approximate and exact grand partition functions using these values of z_{max} are shown in Fig 5.2. The heat capacity projected from the exact grand canonical partition function agrees uniformly with the exact canonical result to within 2 %. Once again the results of the projection on the approximate grand partition function are poor, with an average error of 10 %, and a maximum error of 21 %. The numerical calculations indicate however that if the Chebyschev results display a strong dependence on the cutoff one should not use the method.

Thus, despite the fact that the projected energy agrees to within 4 % with the exact canonical energy on average (see Fig. 5.3), it is clear that the heat capacity compares poorly with the exact canonical result. It is difficult to pinpoint the exact reason for the failure of these straightforward projection techniques. Our results suggest that it is not possible to obtain accurate projected results using the RPA-SPA approximation to the grand partition function, which only takes into account thermal and first order quantum corrections. The inclusion of higher order quantum corrections in the path integral approximation to the grand partition function must therefore be vital in this regard. It may also be necessary to develop a projection technique that takes into account the manner (in this case RPA-SPA) in which the grand partition function is approximated. Such a method would, however, lose its generality, since it requires knowledge of the specific form of the approximation.

Our results seem to indicate that even though the exact grand partition function fully contains the information on the various canonical ensembles, much of this information becomes inaccessible via simple projection techniques when only an approximation, albeit a very good one, to the grand partition function is known.

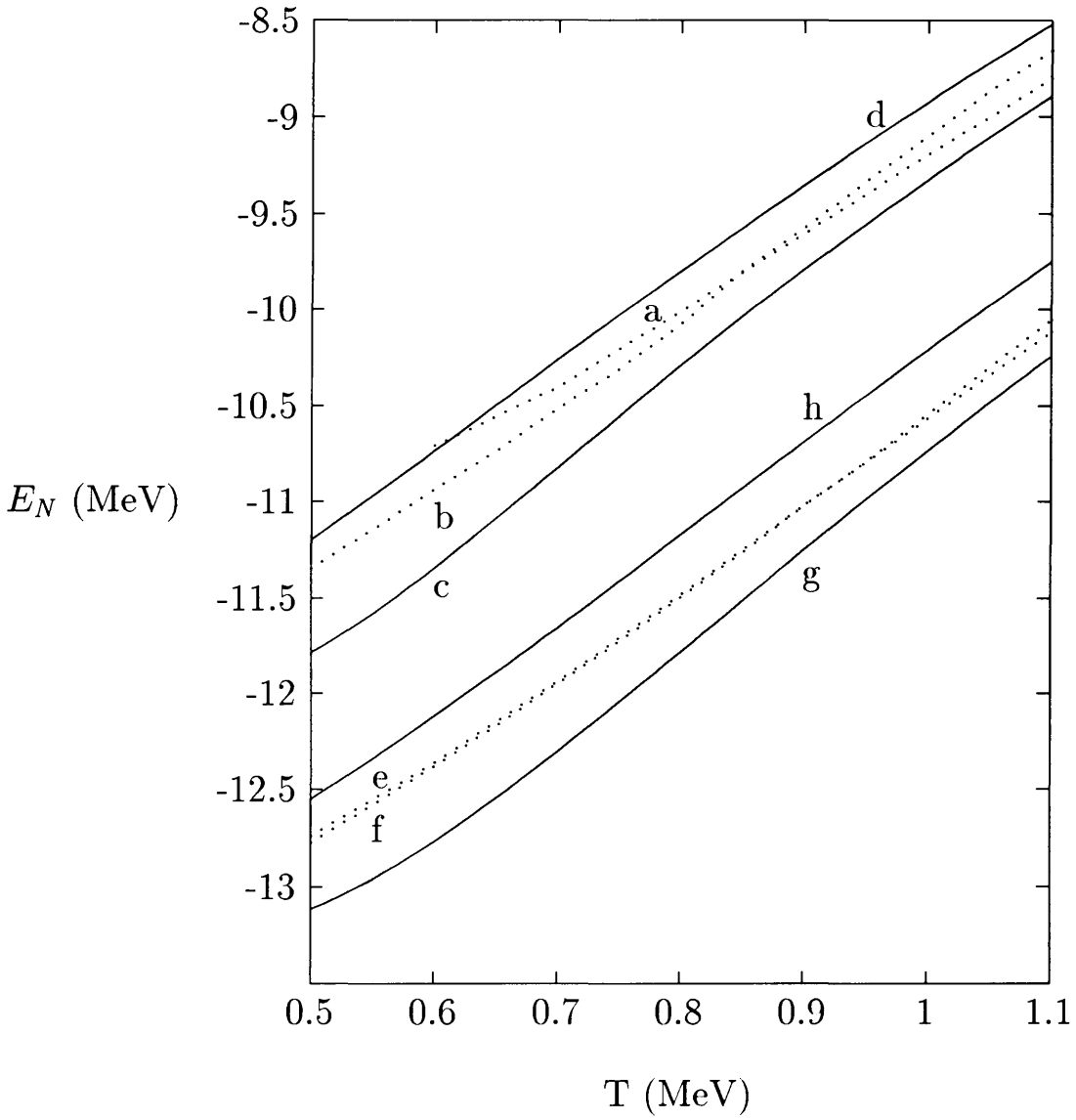

Figure 5.3: The projected energy as a function of temperature, using the "Wick rotation" and Chebyschev expansion methods (dotted lines), and the exact energy calculated in the canonical and grand canonical ensembles (solid lines). The results for $N = 6$ are labelled a, b, c, d, and the results for $N = 8$ are labelled e, f, g, h, respectively.

Chapter 6

Summary and Conclusions

In this dissertation I have analytically solved the standard BCS gap equation *without* the restriction that the interaction width of the intermediating bosons be small with respect to the Fermi energy. One obtains the universal form for BCS gap parameter $\frac{\Delta}{E_F}$ (see chapter 3)

$$\delta \equiv \frac{\Delta}{E_F} = f_D(\nu) \exp\left(-\frac{1}{\lambda}\right), \tag{6.1}$$

for arbitrary width, $\nu \equiv \frac{\hbar\omega_D}{E_F}$, of the BCS model interaction, with the analytical dimension-dependent functions $f_D(\nu)$ given in Table 3.1 [19, 20], and the coupling parameter λ given by

$$\lambda = v_0 N(0) \tag{6.2}$$

as before. Equation (6.1) indicates clearly that, at least in the weak coupling limit, the essential singularity in coupling cannot be ascribed to the quasi-two-dimensional nature of phononic superconductivity implied by the limit $\nu \ll 1$. Furthermore, with this extension, the pairing mechanism in the BCS model is no longer restricted to phonons, which are limited by the Debye frequency. At least in the weak coupling limit, other candidates for the intermediating bosons may be considered. Also, since the interaction is not confined to a narrow shell about the Fermi energy, the model is now applicable to systems which are not quasi-2D in nature.

By comparing the functional integral representation of the partition function with the Landau order parameter representation, one is led to propose

the expectation value of the pairing potential, $\mathcal{G}$, as the order parameter of the system, rather than the BCS energy gap Δ [25]. In chapter 4 it was shown that, not only are the conceptual difficulties arising from the conventional choice of Δ as the order parameter resolved, but my numerical calculations indicate that the use of $\mathcal{G}$ provides a better prediction of the expectation value of the pairing potential (see Fig. 4.1), and of the critical temperature T_c given by the position of the peak in the heat capacity (see Fig 4.2). The comparison of the Landau representation of the partition function with the path integral representation evaluated in the SPA, also yields physical insight into the nature of the static path approximation [25].

The properties of small systems need to be calculated in the canonical, rather than the grand canonical ensemble. As a test of canonical projection methods, and since exact calculations are often impossible, canonical number projection was performed on an approximate grand partition function in the $i_{\frac{13}{2}}$ model in chapter 5. Nuclei with six and eight pairing nucleons were considered. I employed two projection methods, namely a contour integral method, and a Chebyschev series inversion method. The grand partition function was approximated using the RPA-SPA functional integral approximation, which includes thermodynamic and small-amplitude quantum fluctuations (see chapter 4). The energy was found to be insensitive to the choice of ensemble, with very little difference between the energy calculated in the canonical and grand canonical ensemble. Thus, if only the energy is required, canonical projection is in most cases unnecessary. The heat capacity, however, shows an appreciable difference when calculated in the canonical versus the grand canonical ensemble. Although this difference is smaller than the magnitude of the grand canonical number fluctuations would lead one to expect, it is not negligible, and canonical number projection has therefore been performed. The projected canonical results for the heat capacity (see Figs. 5.2 and 5.1) turned out to be extremely disappointing, particularly since the RPA-SPA path integral approximation used for the grand partition function is very good. The minimum average difference between the projected results and the exact canonical heat capacity is 10 %, which is of the same order of magnitude as the difference between the exact canonical and grand canonical heat capacity.

Since it may be argued that the poor projected results are the result of numerical error, I have checked the numerical error due to the projection methods by performing the projection on the exact grand canonical partition

function, and comparing with the exact canonical results. For the contour integral method or "Wick rotation" the numerical error is entirely negligible. This method provides numerically stable and therefore reliable results. The Chebyschev method, although numerically somewhat unstable for six particles in the high temperature region, does not introduce numerical errors nearly large enough to account for the huge errors in the projected results. In principle, the exact grand canonical partition function contains all the information on the various canonical ensembles. These results suggest this information is lost, or at least inaccessible via simple projection techniques, when only a good approximation to the grand partition function is known.

Appendix A

The $i_{\frac{13}{2}}$ Model

In this schematic model for heavy nuclei [8] one focuses on the particles in the $i_{\frac{13}{2}}$ shell with the pairing Hamiltonian given by

$$\hat{H} = \sum_k \epsilon_k \left(a_k^\dagger a_k + a_{\overline{k}}^\dagger a_{\overline{k}} \right) - G \sum_{kk'} a_k^\dagger a_{\overline{k}}^\dagger a_{\overline{k'}} a_{k'} \,. \tag{A.1}$$

Here $G > 0$ is the pairing constant, $k = 1, 2, \ldots, 7$ labels the seven single-nucleon states $\mid i_{\frac{13}{2}}, m >$ where $m - \frac{1}{2}$ is an even integer, with m the projection of the spin on the z-axis. $\overline{k}$ then labels the time reversed state of k, i.e. $\mid i_{\frac{13}{2}}, -m >$. Setting $m = \frac{17}{2} - 2k$, the single particle energies $\epsilon_k = \epsilon_{\overline{k}}$ are given by

$$\epsilon_k = \kappa \frac{3m^2 - j(j+1)}{j(j+1)} \tag{A.2}$$

with $j = \frac{13}{2}$ and $\kappa = 2.0$ MeV. The pairing constant G has been chosen as 0.448 MeV [8] so that the BCS energy gap for six nucleons at zero temperature is 1.0 MeV.

This particular model has been chosen since, besides being a quasi-realistic model of certain nuclei, it yields exact canonical and grand canonical results in a relatively simple manner. Consider the canonical partition function Z_N for N particles

$$Z_N(\beta) = \sum_{E_r} g(E_r) \exp\left(-\beta E_r\right) , \tag{A.3}$$

with E_r the N-particle energy eigenvalues, $g(E_r)$ the degeneracy of the eigenvalue E_r and $\beta = \frac{1}{k_B T}$ the inverse temperature. We choose as a basis the eigenstates of the non-interacting Hamiltonian. Each of these states corresponds to a particular distribution of the N particles over the 14 available unperturbed single particle levels. In this basis, we construct a matrix representation H of the Hamiltonian $\hat{H}$, with dimension

$$D = C_N^{14} . \tag{A.4}$$

Here the combinatorial factor

$$C_q^p = \frac{p!}{(p-q)!\, q!} \tag{A.5}$$

specifies the number of ways to distribute q identical objects over p different boxes, with at most one object per box. The many body energies $\{E_r\}$ are now obtained by diagonalizing the matrix H. Note here that since the Hamiltonian conserves the *number of pairs*, the problem simplifies to a diagonalization of the submatrices H_m corresponding to a fixed number m of pairs. Furthermore, since the Hamiltonian is diagonal in spin, and since $\epsilon_k = \epsilon_{\bar{k}}$, we need only consider distributing the $N - 2m$ unpaired particles over the seven states with positive spin. Let H'_m denote the matrix in this reduced subspace. Each eigenvalue of H'_m then has a degeneracy 2^{N-2m}.

Let D_m denote the dimension of the subspace spanned by states with m pairs. Then

$$D_m = C_{N-2m}^7 \times 2^{N-2m} \times C_m^{7-(N-2m)} . \tag{A.6}$$

Here C_{N-2m}^7 represents to the number of ways to distribute the $N - 2m$ unpaired particles over the seven available levels with positive spin, 2^{N-2m} is the degeneracy factor mentioned above, and $C_m^{7-(N-2m)}$ corresponds to number of ways to pick the m paired levels from the $7 - (N - 2m)$ levels not occupied by the unpaired particles.

There is a further blocking of H'_m due to the fact that Hamiltonian clearly does not alter the distribution of the $N - 2m$ unpaired particles, so that this distribution is "conserved" within a particular pair number subspace. Thus, each subspace with fixed number of pairs m decomposes into C_{N-2m}^7 sub-subspaces, each corresponding to a particular distribution, labelled s, of the $N - 2m$ unpaired particles over the 7 available levels. Therefore, instead of

diagonalizing the submatrices H'_m, one simply diagonalizes the subsubmatrices H^s_m. These matrices are easily coded and diagonalized numerically, yielding the required energy eigenvalues, with degeneracies 2^{N-2m}, of the system.

To illustrate this procedure, consider the case $N = 4$. The full Hamiltonian in the single particle distribution basis has the form

$$\begin{bmatrix} \begin{bmatrix} H_0 \\ C_4^7 \times 2^4 \times C_0^3 \\ = \ 35 \times 16 \times 1 \end{bmatrix} & \emptyset & \emptyset \\ \emptyset & \begin{bmatrix} H_1 \\ C_2^7 \times 2^2 \times C_1^5 \\ = \ 21 \times 4 \times 5 \end{bmatrix} & \emptyset \\ \emptyset & \emptyset & \begin{bmatrix} H_2 \\ C_0^7 \times C_2^7 \times 2^0 \\ = \ 1 \times 1 \times 21 \end{bmatrix} \end{bmatrix} \tag{A.7}$$

where the dimension of each submatrix H_m has been indicated. Rather than having to diagonalize this matrix, one need only consider the problem of diagonalizing the reduced submatrices H'_m, given by

$$\begin{bmatrix} H'_0 \\ C_4^7 \times C_0^3 \\ = \ 35 \times 1 \end{bmatrix} \ , \ (g = 2^4 = 16)$$
$$\begin{bmatrix} H'_1 \\ C_2^7 \times C_1^5 \\ = \ 21 \times 5 \end{bmatrix} \ , \ (g = 2^2 = 4)$$
$$\begin{bmatrix} H'_2 \\ C_0^7 \times C_2^7 \\ = \ 1 \times 21 \end{bmatrix} \ , \ (g = 2^0 = 1) \tag{A.8}$$

Here the dimension and degeneracy g of each reduced submatrix H'_m has been indicated. Consider now the submatrix H'_0 corresponding to those states with no pairs. Since the Hamiltonian doesn't mix states with different single particle distributions s, the submatrix H'_0 is already diagonal. The many body eigenvalue E^0_s corresponding to a particular distribution s is simply given by the sum over the energies of the single particle levels occupied in

that distribution. Thus

$$E_s^0 = \sum_{k\,[s]} \epsilon_k \,, \tag{A.9}$$

where the sum goes over the levels occupied in the distribution s. Each of these eigenvalues has a degeneracy $2^4 = 16$. Thus the contribution to the partition function Z_4 from the states with zero pairs is given by

$$Z_4^0 = 16 \sum_s e^{-\beta E_s^0} \tag{A.10}$$

The submatrix H_1' corresponds to states with one pair. There are two independent particles to be distributed over seven levels in $C_2^7 = 21$ ways, labelled s_1 to s_{21}. Then, since the Hamiltonian does not affect the distribution s_i, the matrix H_1' may be cast in the block diagonal form

$$\begin{bmatrix} [H_1^{s_1}] & \emptyset & \emptyset & \cdots & \cdots & \emptyset \\ \emptyset & [H_1^{s_2}] & \emptyset & \cdots & \cdots & \emptyset \\ \emptyset & \emptyset & [H_1^{s_3}] & \cdots & \cdots & \emptyset \\ \vdots & \vdots & \vdots & & & \vdots \\ \vdots & \vdots & \vdots & & [H_1^{s_{20}}] & \emptyset \\ \emptyset & \emptyset & \emptyset & \cdots & \emptyset & [H_1^{s_{21}}] \end{bmatrix} . \tag{A.11}$$

Here each subsubmatrix $H_1^{s_i}$ has dimension $C_1^5 = 5$. The factor $C_1^5 = 5$ arises from the five possible ways to pick the paired level, so that, for each distribution s_i, one is left with a simple 5×5 matrix to code and diagonalize. Denote the five eigenvalues of this matrix by $E_k^{s_i}$, where $k = 1, 2, \ldots, 5$, each eigenvalue having a degeneracy $2^2 = 4$. Then the states with one pair make a contribution

$$Z_4^1 = 4 \sum_{i=1}^{21} \sum_{k=1}^{5} e^{-\beta E_k^{s_i}} \tag{A.12}$$

to the partition function for $N = 4$ particles.

The submatrix H_2' corresponds to the subspace spanned by states with two pairs. Here there are no independent particles left to distribute, so that the symmetries of the Hamiltonian exploited above cannot be utilized. Therefore the matrix H_2' has to be coded and diagonalized explicitly, yielding

eigenvalues E_i with $i = 1, 2, \ldots, 21$, which make a contribution

$$Z_4^2 = \sum_{i=1}^{21} e^{-\beta E_i} \tag{A.13}$$

to the partition function. The full canonical partition function for four particles is then simply given by

$$Z_4 = Z_4^0 + Z_4^1 + Z_4^2 . \tag{A.14}$$

Given the exact canonical partition functions, the exact grand canonical partition function $\mathcal{Z}$ as a function of β and the chemical potential μ is simply

$$\mathcal{Z}(\beta, \mu) = \sum_N \exp(\beta \mu N) Z_N . \tag{A.15}$$

All thermodynamic properties of the system, such as the energy and the specific heat, now follow in straightforward manner in either the canonical or grand canonical ensemble from the relevant partition function.

Bibliography

[1] H. K. Onnes, *Commun. Phys. Lab. Univ. Leiden, Suppl.* **34b** (1913).

[2] J. Bardeen, L. N. Cooper and J. R. Schrieffer, *Phys. Rev.* **108**, 1175 (1957).

[3] D. R. Tilley and J. Tilley, *Superfluidity and Superconductivity*, Adam Hilger, Bristol (1990).

[4] P. W. Anderson and P. Morel, *Phys. Rev.* **123**, 1911 (1961).

[5] R. Balian and N. R. Werthamer *Phys. Rev.* **131**, 1553 (1963).

[6] A. B. Migdal, *Nucl. Phys.* **13**, 655 (1959).

[7] M. Hoffberg, A. E. Glassgold, R. W. Richardson and M. Ruderman, *Phys. Rev. Lett.* **24**, 775 (1970).

[8] A. L. Goodman, *Phys. Rev. C* **29**, 1887 (1984).

[9] W. A. Little, *Phys. Rev A* **134**, 1416 (1964).

[10] D. Jérome, A. Mazuad, M. Ribault and K. Bechgaard, *J. Physique Lett.* **41**, L95 (1980).

[11] F. Steglich, J. Aarts, C. D. Bredl, W. Lieke, D. Meschede, W. Franz and H. Schäfer, *Phys. Rev. Lett.* **43**, 1892 (1979).

[12] J. G. Bednorz and K. A. Muller, *Z. Physik* **B64**, 189 (1986).

[13] C. W. Chu, L. Gao, F. Chen, Z. J. Huang, R. L. Meng and Y. Y. Xue, *Nature* **365**, 323 (1993).

[14] J. R. Schrieffer, X.-G. Wen and S.-C. Chang,
Physica **C153-155**, 21 (1988).

[15] W. Pint and E. Schachinger, *Phys. Rev. B* **43**, 7664 (1991).

[16] P. W. Anderson, G. Baskaran, Z. Zou, J. Wheatley, T. Hsu, B. S. Sastry, B. Doucot and S. Liang, *Physica* **C153-155**, 527 (1988).

[17] "A Dialogue on the theory of high T_c", P. W. Anderson and J. R. Schrieffer, *Physics Today* **44**, 54 (1991).

[18] P. Fulde, *Physica* **C153-155**, 1769 (1988).

[19] D. M. Eagles, *Phys. Rev.* **164**, 489 (1967).

[20] D. M. van der Walt, R. M. Quick and M. de Llano, *J. Math. Phys.* **43** 3980 (1993).

[21] S. Jin, T. H. Tiefel, R. C. Sherwood, R. B. Dover, M. E. Davis, G. W. Kammlot and R. A. Fastnacht, *Phys. Rev. B* **37**, 7850 (1988).

[22] J. W. Ekin et al., *J. Appl. Phys.* **62**, 4821 (1987).

[23] P. Chaudhari, J. Manhart, D. Dimos, C. C. Tsuei, J. Chi, M. M. Oprysko and M. Scheuermann, *Phys. Rev. Lett.* **60**, 1653 (1988).

[24] F. Solms, N. J. Davidson, H. G. Miller, R. M. Quick and H. L. Gaigher, *Phys. Lett. A* **170**, 137 (1992).

[25] M. Marinus, H. G. Miller, R. M. Quick, F. Solms and D. M. van der Walt, *Phys. Rev. C* **48**, 1713 (1993).

[26] P. Ring and P. Schuck *The Nuclear Many-Body Problem*,
Springer-Verlag, New York (1980).

[27] D. M. van der Walt and R. M. Quick, "Canonical number projection in a simple nuclear model", Accepted for publication in *Phys. Rev. C* (1994).

[28] H. Fröhlich, *Phys. Rev.* **79**, 845 (1950).

[29] L. N. Cooper, *Phys. Rev.* **104**, 1189 (1956).

[30] N. N. Bogoliubov, *Sov. Phys. JETP* **7**, 41 (1958).

[31] A. L. Fetter and J. D. Walecka, *Quantum Theory of Many-Particle Systems*, McGraw-Hill, New York (1971).

[32] W. Meissner and R. Oschenfeld, *Naturwiss.* **21**, 787 (1933).

[33] C. Esebbag, J. M. Getino, M. de Llano, S. A. Moszkowski, U. Oseguera, A. Plastino and H. Rubio, *J. Math. Phys.*, **33** 1221 (1992).

[34] M. Casas, C. Esebbag, A. Extremera, J. M. Getino, M. de Llano, A. Plastino and H. Rubio, *Phys. Rev. A* **44**, 4415 (1991).

[35] C. Esebbag, M. de Llano and R. M. Quick, *Phys. Rev. B* **B47**, 11512 (1993).

[36] J. Hubbard, *Phys. Rev. Lett.* **3**, 77 (1959).

[37] R. L. Stratonovich, *Soviet Phys. Doklady* **2**, 416 (1958).

[38] R. P. Feynman and A. R. Hibbs, *Quantum Mechanics and Path Integrals*, McGraw-Hill, New York (1965).

[39] G. Puddu, P. F. Bortignon and R. A. Broglia, *Phys. Rev. C* **42**, 1831 (1990).

[40] G. Puddu, P. F. Bortignon and R. A. Broglia, *Ann. Phys.* **206**, 409 (1991).

[41] B. Mühlschlegel, *J. Math. Phys.* **3**, 522 (1962).

[42] A. L. Goodman, *Phase Structure of Strongly Interacting Matter*, Ed. J. Cleymans, Springer-Verlag, Heidelberg (1990).

[43] R. K. Pathria, *Statistical Mechanics*, Pergamon Press, Oxford (1992).

[44] R. Rossignoli, P. Ring and N. Dinh Dang, *Phys. Lett. B* **297**, 9 (1992).

[45] N. Dinh Dang, P. Ring and R. Rossignoli, *Phys. Rev. C* **47**, 606 (1993).

[46] R. Rossignoli, A. Ansari and P. Ring, *Phys. Rev. Lett.* **70**, 1061 (1993).

[47] B. Mühlschlegel, *Surface Science* **106**, 350 (1981).

[48] M. Abramowitz and I. A. Stegun (ed.), *Handbook of Mathematical Functions*, National Bureau of Standards, Washington (1964).